European Union’s Seventh Framework Programme
Grant Agreement Nº: 603521

Project Acronym: **PREFACE**

Project full title: **Enhancing prediction of tropical Atlantic climate and its impacts**

Instrument: Collaborative Project

Theme: ENV.2013.6.1-1 – *Climate-related ocean processes and combined impacts of multiple stressors on the marine environment*

Start date of project: 1 November 2013 Duration: 48 Months

# Deliverable Reference Number and Title:

# D8.1

# ”Interdependence between biases in the Tropical Atlantic and in other regions”

**Lead work package for this deliverable: WP8**

**Lead beneficiary for this deliverable: UCM**

**Due date of deliverable: 31/10/2015**

**Actual submission date: 06/11/2015**

| **Project co-funded by the European Commission within the Seven Framework Programme (2007-2013)** | | |
|---|---|---|
| **Dissemination Level** | | |
| **PU** | Public | X |
| **PP** | Restricted to other programme participants (including the Commission Services) | |
| **RE** | Restricted to a group specified by the Consortium (including the Commission Services) | |
| **CO** | Confidential, only for members of the Consortium (including the Commission Services) | |

**Contribution to project objectives** – with this deliverable, the project has contributed to the achievement of the following objectives (see Annex I / DOW, Section B1.1.):

| N.º | Objective | Yes | No |
|---|---|---|---|
| 1 | Reduce uncertainties in our knowledge of the functioning of Tropical Atlantic (TA) climate, particularly climate-related ocean processes (including stratification) and dynamics, coupled ocean, atmosphere, and land interactions; and internal and externally forced climate variability. | X | |
| 2 | Better understand the impact of model systematic error and its reduction on seasonal-to-decadal climate predictions and on climate change projections. | X | |
| 3 | Improve the simulation and prediction TA climate on seasonal and longer time scales, and contribute to better quantification of climate change impacts in the region. | X | |
| 4 | Improve understanding of the cumulative effects of the multiple stressors of climate variability, greenhouse-gas induced climate change (including warming and deoxygenation), and fisheries on marine ecosystems, functional diversity, and ecosystem services (e.g., fisheries) in the TA. | X | |
| 5 | Assess the socio-economic vulnerabilities and evaluate the resilience of the welfare of West African fishing communities to climate-driven ecosystem shifts and global markets. | | X |

## Authors of this deliverable:

B. Rodríguez-Fonseca (1); Teresa Losada (1); Irene Polo (1); Elsa Mohino (1); Antonio Castaño(1); Julian Villamayor (1); Marta Martín-Rey (2); Noel Keenlyside (3); Mojif Latif (4); W Park (4); T Park (4); P. Greatbach (4); J. Shonk (5); S. Woolnough (5); T. Toniazzo (6); Shunya Koseki (3)

(1) UCM, (2) UPMC, (3) UiB, (4) GEOMAR, (5) UREAD, (6) UniRes

## Deviation from planned efforts for this deliverable:

There has been two deviations from the original plan:

1. Beneficiary UCM has taken the lead on this deliverable. It was more efficient for them to perform the analysis of the biases in CMIP5 models, as they had data and analysis software already in place. Beneficiary UNN were then able to pursue an analysis of decadal variability in the South Atlantic; this class of variability was only identified in the project work, and has not been studied before. Thus, UNN transferred 12 PM to WP9 and contributed to D9.2.

2. UCM and UiB have made an early start on the planned sensitivity experiments (MS27 due at month 42), and preliminary results are presented here. Neither of these has caused a delay in this deliverable. Some sensitivity experiments were planned to do in coordination with Meteo-France

and UPMC. The experiments have been done their contribution is going to be postpone to the next coordinated effort.

## Report on the deliverable:

**D8.1 main objective:** Interdependence between biases in the Tropical Atlantic and in other regions: Report on results from the analysis of the CMIP5 and seasonal to decadal integrations and from new model sensitivity tests, targeting the influence of remote biases on the Tropical Atlantic, and vice versa. Particular focus will be given on of interactions between processes in the tropical Atlantic and the tropical Pacific

### Introduction

Analysis of model systematic errors has generally focused on local processes. However, several recent studies have begun to explore the non-local impact of errors. For example, Wang et al. (2014) have linked errors in surface temperature across the globe to errors in the strength of the Atlantic Meridional Overturning Circulation. Tropical rainfall and SST errors have also been linked to errors in southern hemisphere cloud biases (Hwang and Frierson, 2013; Li and Xie, 2014). Furthermore, the dominant characteristics of tropical model errors have been studied. To first order the error in tropical SST is a uniform pattern (Li and Xie, 2012). The second order pattern shows errors in equatorial Pacific and Atlantic cold tongues (Li and Xie, 2012) that are associated with the dominant error pattern in tropical precipitation (Li and Xie, 2014). Tropical Pacific errors have been shown to impact simulation of the tropical Atlantic (Tozuka et al., 2011). The aim of this study is to address the less known effects of the large mean biases in the tropical Atlantic on the simulation of the Pacific and other regions.

In this way, in the present deliverable, a summary of the main efforts done in the framework of PREFACE around the remote influence on bias and variability is presented.

First, the influence of remote systematic errors on the tropical Atlantic bias and variability is studied using seasonal integrations from SPECS and the CMIP5 Pi-control simulations. Then, some hypotheses are posed and results from sensitivity experiments done in coordination between UCM and UiB are described (section 1).

Secondly, the influence of tropical Atlantic bias on the representation of the mean state and variability out of the TA is presented using partially coupled experiments. In this way, UCM, UiB and GEOMAR have compared the existing simulations from Rodriguez-Fonseca et al (2009), Polo et al (2015) and Ding et al (2011) to see the effect of restoring the Atlantic sea surface temperature to observations in the mean bias and variability in the rest of the tropical basins (section 2).

**1. To assess the influence of systematic errors in regions remote from the Tropical Atlantic on the Tropical Atlantic mean state, and variability.**

***1.1. To pose hypothesis from the analysis of CMIP5 control runs.***

**Mean state SST variability in CMIP5 models and remote influences.**

**Participants**

Irene Polo (UCM); Julian Villamayor (UCM); Belen Rodríguez-Fonseca (UCM)
Elsa Mohino (UCM); Teresa Losada (UCM)

**<u>Description of Leading modes of SST mean state variability in CMIP5 models</u>**

The methodology followed is the same as in Li and Xie (2012) but applied to the SST mean state in the tropics. The focus is to understand the inter-model variability of tropical SST biases in 18 models from CMIP5 Pi-control simulations (see Table 1a).

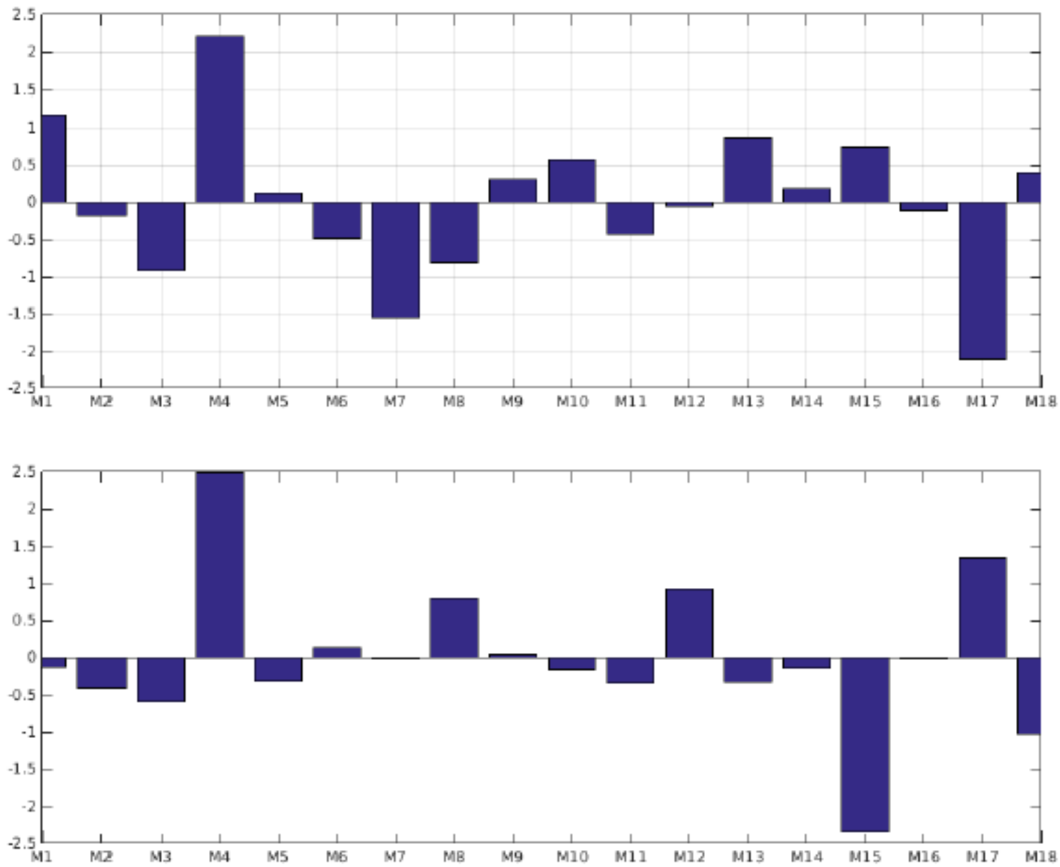


**Figure 1.a.1:** First (top) and second (bottom) principal components of the annual mean tropical (between 30ºS and 30ºN) SST state inter-model variability of 18 CMIP5 models. The PC are standardized.

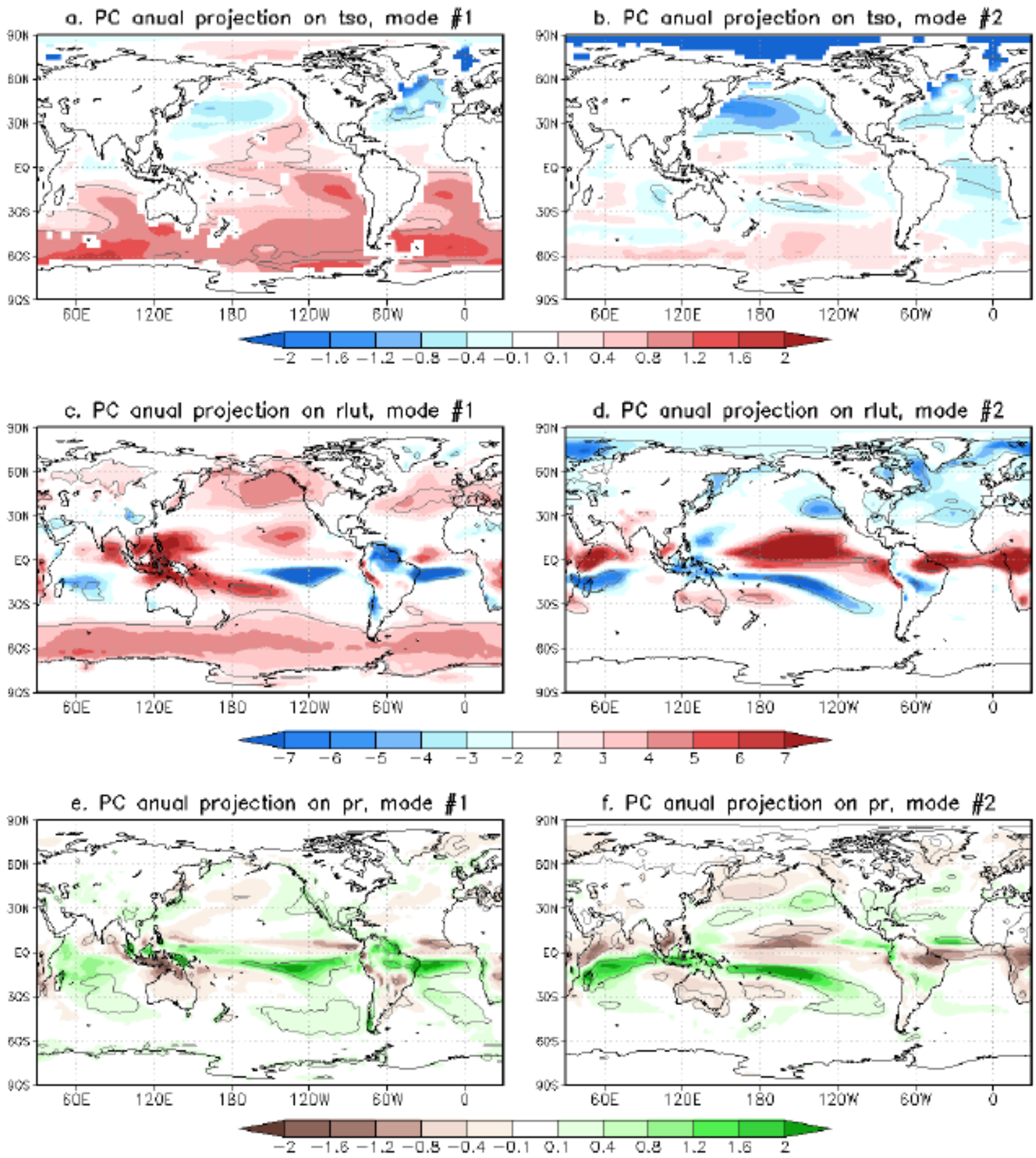


**Figure 1.a.2:** Projections of the annual mean SST (top), ORL (rlut, middle) and precipitation (bottom) of CMIP5 models onto the first (left) and second (right) PC (figure 1) of tropical annual mean SST inter-model variability. Units are ºC per standard deviation of the PC, $Wm^{-2}$ per standard deviation of the PC and mm/day per standard deviation of the PC, respectively. Gray lines indicate statistically significant correlations between the field and the PC (alpha=0.05) using a two-tailed t-test.

To this aim, the deviations in the annual climatology of tropical SSTs (30ºS – 30ºN) for each model with respect to the multi-model average are calculated and an EOF analysis is applied. Thus the scores in the principal components (Figure 1.a.1) represent the factor by which the EOF (Figure 1.a.2, top) must be multiplied to obtain the contribution of a particular model to the associated mode.

The two leading modes account for more than the 40 % of the variance (26 % and 18 % respectively).

For the leading mode, there is a clear connection between the tropical biases and the extratropics (note that the EOF analysis was restricted to the tropics): the warmer (cooler) the model climatology is in the eastern tropical tongues, the less (more) cloudiness (in terms of increasing OLR) is simulated in the southern subtropical oceans and the more southward (northward) the ITCZ is located (figure 1.a.2, left panels). The positive phase of the mode happens in those models that show positive scores in PC1 (figure 1.a.1, top). This result coincides with Li and Xie (2014), when relating the second mode of Pacific rainfall with the bias in the cloudiness of the Southern Hemisphere. This results, also in agreement with Hwang and Frierson (2013), who point to the key impact that the representation of the clouds in the Southern Hemisphere has in the good simulation of the tropical characteristics of climate in models.

Unlike the leading mode, the second one is related to extratropical SST anomalies in the northern hemisphere. However, its main projection on clouds and precipitation is located in the tropics, suggesting that the cloud biases in the tropics are linked the bias in the position/strength of the ITCZ that, in turn, appears to be related to the SST biases in the Northern Hemisphere.

| **Modeling Center (or Group)** | **Institute ID** | **Model Name** | **Nyears/ Resolution** |
|---|---|---|---|
| Canadian Centre for Climate Modelling and Analysis | CCCMA | CanESM2**(M1)** | 996/128x64 |
| National Center for Atmospheric Research | NCAR | CCSM4**(M2)** | 501/288x192 |
| Centre National de Recherches Meteorologiques | CNRM-CERFACS | CNRM-CM5**(M3)** | 850/256 x 128 |
| Commonwealth Scientific and Industrial Research Organization | CSIRO-QCCCE | CSIRO-Mk3.6.0**(M4)** | 500/192x96 |
| NASA Goddard Institute for Space Studies | NASA GISS | GISS-E2-R **(M5)**<br>GISS-E2-H**(M6)** | 550/144x90<br>531/144x90 |

| | | | |
|---|---|---|---|
| NOAA Geophysical Fluid Dynamics Laboratory | NOAA GFDL | GFDL-ESM2G**(M7)**<br><br>GFDL-ESM2M**(M8)** | 500/<br><br>500 |
| Met Office Hadley Centre | MOHC | HadGEM2-CC **(M9)**<br><br>HadGEM2-ES **(M10)** | 240/192x145<br>575/ |
| Institute for Numerical Mathematics | INM | INM-CM4**(M11)** | 500/180x120 |
| Atmosphere and Ocean Research Institute (The University of Tokyo), | MIROC | MIROC-ESM-CHEM **(M14)** | 255/128x64 |
| Atmosphere and Ocean Research Institute (The University of Tokyo), | MIROC | MIROC4h **(M12)**<br><br>MIROC5 **(M13)** | 100/640x320<br>670/256x128 |
| Max Planck Institute for Meteorology | MPI-M | MPI-ESM-LR **(M15)** | 1000/192x96 |
| Meteorological Research Institute | MRI | MRI-CGCM3 **(M16)** | 500/320x160 |
| Norwegian Climate Centre | NCC | NorESM1-M **(M17)** | 501/144x96 |
| Institut Pierre-Simon Laplace | IPSL | IPSL-CM5A-LR **(M18)** | 1000/96x96 |

Table1.a: Models from CMIP5 experiment used in this analysis and observational dataset.

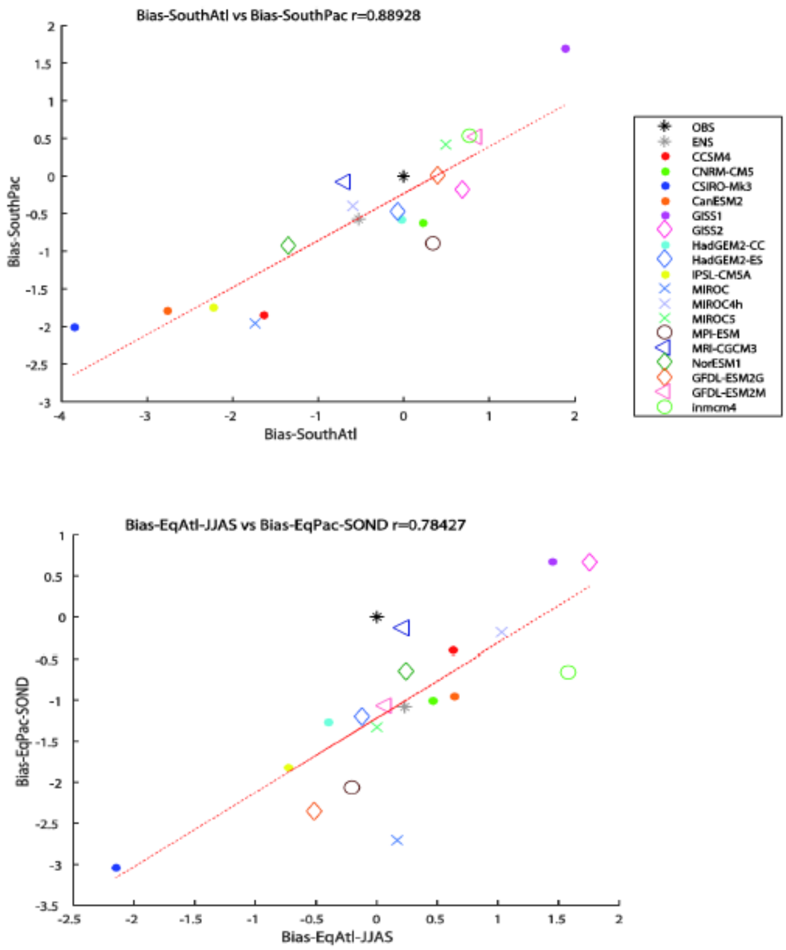


Figure 1.a.3: **Relationship between mean bias at the equator and southern hemisphere.** A) Scatter plots between the mean bias over the south Atlantic and south Pacific annual mean. B) Relationship between the bias over the equatorial Atlantic in boreal summer and the bias over the equatorial Pacific in boreal autumn.

Figure 1.a.3 shows the scatter plots between the bias in the equatorial Atlantic [40W-0; 3S-3N] and Pacific regions [200W-90W; 5S-5N]. It suggests that mean errors in the equatorial band are related: models with warmer (cooler) bias over equatorial Atlantic in boreal summer tend to have warmer (cooler) equatorial Pacific in boreal autumn (panel (a) of Figure 1.a.3). Bias are also related in the southern hemisphere in a similar way. Even though the biases over the Equatorial regions are highly related, causality is very difficult to identify. In the next section the interaction between mean bias and variability is discussed.

## Description of the interaction between bias and variability in CMIP5 models (Polo et al., 2015a)

Interannual to decadal modes of SST variability have been analysed in the CMIP5 models (see table1b) in Pi-Control simulations.

The leading modes of interannual (decadal) variability of SST are determined by calculating the Principal Component of the monthly (annual) SST anomalies for each model after linearly detrending the data (and filtering at decadal timescales). Because each model can have different seasonality from the rest of them, when performing the interannual analysis, all months are chosen.

The models' skill in representing the spatial configuration of each mode is analysed by means of Taylor diagrams, using as the reference the observed spatial pattern. To evaluate the possible relationship between such skill and the model bias, the annual SST bias of the model has been regressed onto the time series of the correlation scores between the simulated and observed patterns.

### -Interannual Variability

The structure of the spatial patterns of the leading modes of variability simulated differ among models. In general the models change the location of the maximum of these structures and, in particular, the longitude of the maximum amplitude in the leading mode of tropical Pacific variability (1TPV) and the latitude of the maximum amplitude in the leading mode of tropical Atlantic variability (1TAV), which are biased to the east and the south respectively (not shown).

Figure 1.a.4 shows the first mode of variability for the Tropical Pacific (1TPV) in the observations together with the Taylor diagram that quantifies the skill of the different models in simulating the spatial pattern associated with the mode. Also, the seasonality of the mode is represented. The models simulate quite well both the spatial pattern and the seasonality (boreal winter) of the Pacific Niño. However, all models show less explained variance than observations ranging from 24% to 55%)

In turn, three different modes describe the variability of the tropical Atlantic ocean (figures 1.a.5 and 1.a.6), being the first and the third, those associated with the two configurations of the equatorial Atlantic Niño (basin-wide and equatorial mode, Martin-Rey et al., 2015). The second mode corresponds to the NTA variability (Meridional mode-like, not shown). The seasonality is comprised between spring and autumn for the leading mode, while for the third mode it occurs mainly in boreal summer, although explaining less variance. The percentage of variance explained by each mode varies among models (in a range of 21% to 42% in 1TAV and 6% to 13% in 3TAV, being the observed modes 35% and 9% respectively).

The possible relationship between the models' ability to simulate the SST Tropical Variability Modes and the mean bias is addressed by means of regression analysis. On the one hand, for each variability mode the annual SST bias of the models is regressed onto the correlation score obtained in the Taylor diagram. On the other, the same annual SST bias field is regressed onto the time series built with the fraction of variance explained by that mode in each model.

Figure 1.a.4 (bottom left) shows that models with colder SSTs over the central-west equatorial, present a Pacific Niño that explains more variability. This could be related with the fact that cooler models over the equatorial Pacific tend to have a shallow thermocline in the central- west Pacific which is known to affect the feedbacks that create more westward extensive Niños (Dong and Sutton, 2007; Shonk et al., 2015). More fraction of variance is also related to a cooler SubPolar Gyre (figure 1.a.5, bottom left), suggesting that models with weaker AMOC enhance equatorial Pacific variability, in agreement with previous results with water hosing experiments (Wang et al., 2014; Dong and Sutton, 2007).

Figure 1.a.4 (bottom right) indicates that models with warmer southern hemisphere SSTs (similar to mode 1 in figure 1.a.2 top) present a more realistic spatial configuration of the Pacific Niño.

In relation to the Atlantic, a cooler southern hemisphere (less bias over there) relates to more variability of 1TAV and better spatial representation of 3TAV (figures 1.a.5 a, and 1.a.6 e). It should be noted that this pattern is also similar to mode 1 in Figure 1.a.2 (top).

Models with less bias over the southern tropics (i.e. negative anomalies), represent better the 3TAV and also present more fraction of explained-variance for 1TAV and 1TPV. This could imply that for negative bias, models could perform better the thermocline feedbacks over TA (3TAV) but also more variance in 1TAV could be due to more variance in the equatorial Pacific (1TPV) impacting though heat fluxes (Polo et al., 2013). We will need to further investigate this with more thermodynamical variables such as Ocean Heat Content and wind stress.

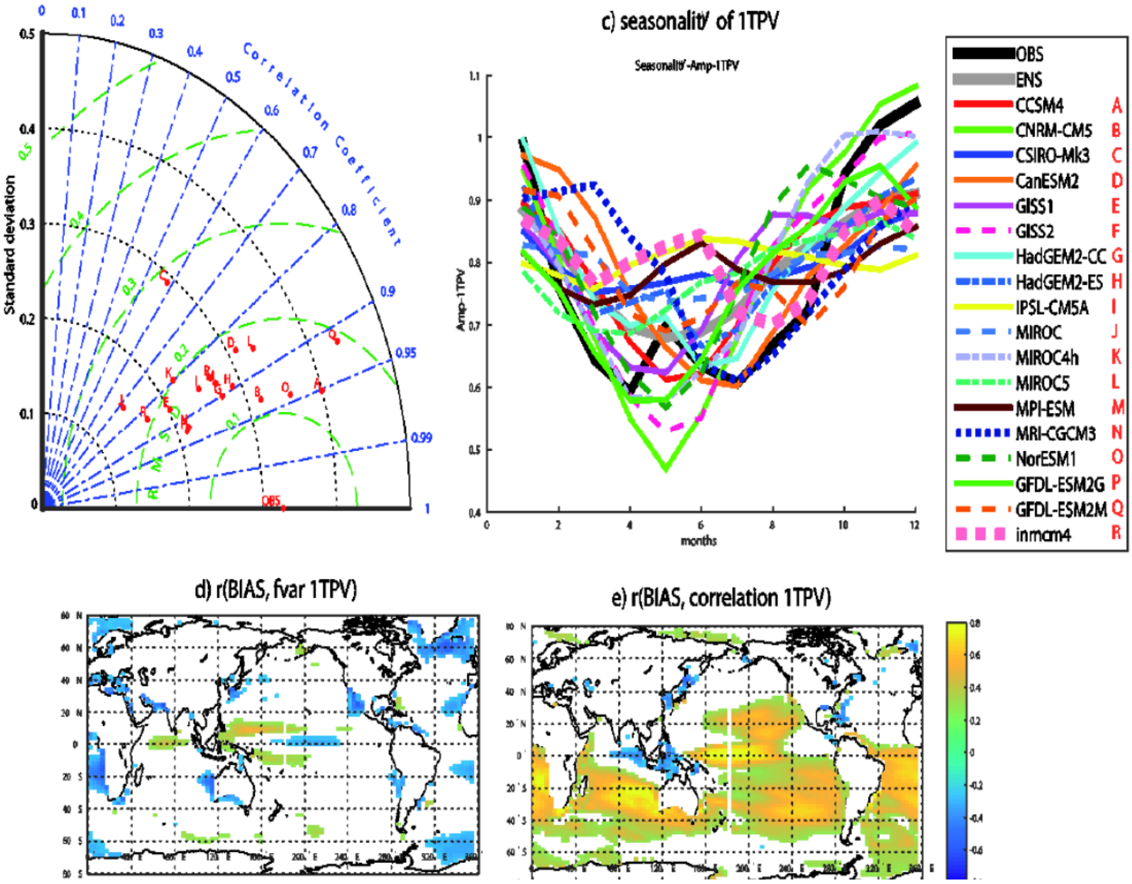


**Figure 1.a.4**: **(a)** Leading mode of observed tropical Pacific Variability **(b)** Taylor diagram comparing the leading mode of TPV pattern of SSTA from observed HadISST1 data (dot on x-axis) against the reproduced by CMIP5 models (red dots from 1 to 17 in the table at right) from control simulations. **(c)** seasonality of the 1TPV for each model and the observations **(d)** correlation between biases of the annual-mean SST of the 17 CMIP5 models and the fraction of variance explained for the 1TPV of each model. **(e)** correlation between biases of the annual-mean SST of the 17 CMIP5 models and the index of correlation coefficients between the observed and the simulated 1TPV patterns represented in the Taylor diagram above.

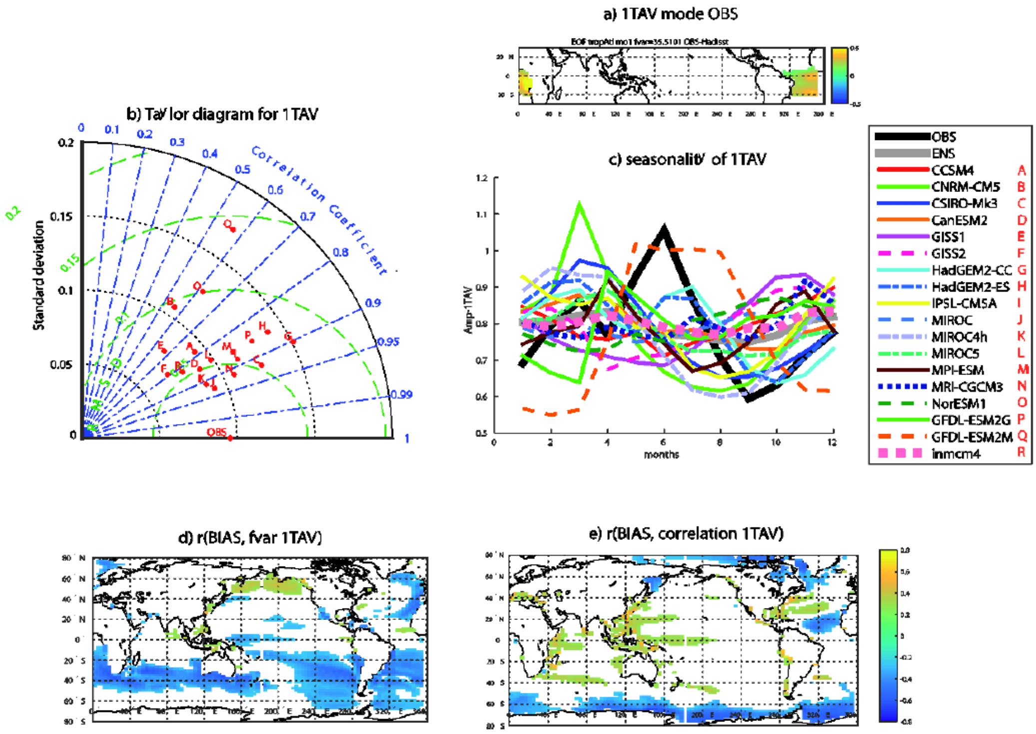


**Figure 1.a.5**: Same as Figure 1.a.4 but for the leading mode of Tropical Atlantic Variability (basin-wide like mode, Martin-Rey et al., 2015).

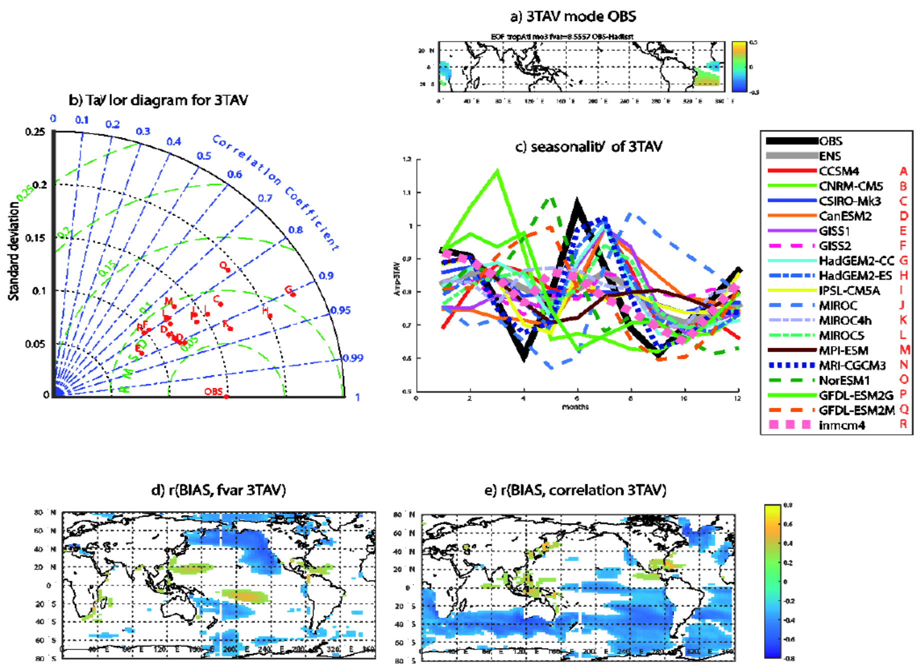


**Figure 1.a.6**: Same as 1.a.4 but for the third mode of Tropical Atlantic Variability (equatorial mode, Nanmchi et al., 2011).

### -Decadal Variability

The same analysis has been carried out to find out whether the bias of CMIP5 models (Taylor et al., 2012) is related to their skill in reproducing the decadal to multidecadal sea surface temperature anomalies (SSTA) patterns. As shown in Villamayor and Mohino (2015) (hereinafter referred to as VM15), the Interdecadal Pacific Oscillation (IPO) is robustly reproduced by CMIP5 in both the historical simulations of the 20$^{th}$ Century and in the preindustrial control (piControl) unforced runs. A Taylor diagram (Figure 1.b.8.a) is computed to compare the IPO patterns of the annual-mean SSTA of the 17 CMIP5 models analyzed in VM15 with the observed, using HadISST1 (Rayner et al., 2003) database.

The Taylor diagram shows that many models reproduce an IPO pattern with a distribution of SSTA similar to the observed one (Figure 1.a.7.a), similarly in both the historical and piControl simulations (only Pi-control one are shown). The pattern averaged among all the models is strongly correlated with the observed (roughly r=0.7). The standard deviation provides an idea of the amplitude of the SSTA projected in the IPO patterns and show that the values from the models tend to group around the observed one. This result supports the conclusion in VM15 that CMIP5 models have a significant ability to reproduce the IPO pattern. But is this skill related to the bias of the models? The regression pattern in Figure 1.a.7, made with the 17 maps of the SSTA bias of the models projected onto the correlation indices of the observed against the simulated IPO patters (represented in the Taylor diagram), suggests that the models that reproduce an IPO pattern closer to the observed one reproduce cooler climatological SSTA in the southern than in the northern hemisphere. More in detail, there are significant negative climatological SSTA southward from 20ºS in all the oceans, extending to tropical latitudes in the South Atlantic and to the tropical Pacific, especially close to South America. In the northern hemisphere there are positive climatological anomalies in the northern Pacific and Atlantic basins. On the one hand, such pattern is reminiscent of the pattern shown in the figure 1.b of Wang et al. (2014), in which they highlight the relationship between the SSTA bias of CMIP5 models and the reproduced Atlantic meridional overturning circulation (AMOC). On the other, the pattern is also similar to the one in Fig. 1.a.2 (top left) which would suggest a possible link with cloud coverage in the southern extratropics. Further research will be devoted to evaluate both possibilities.

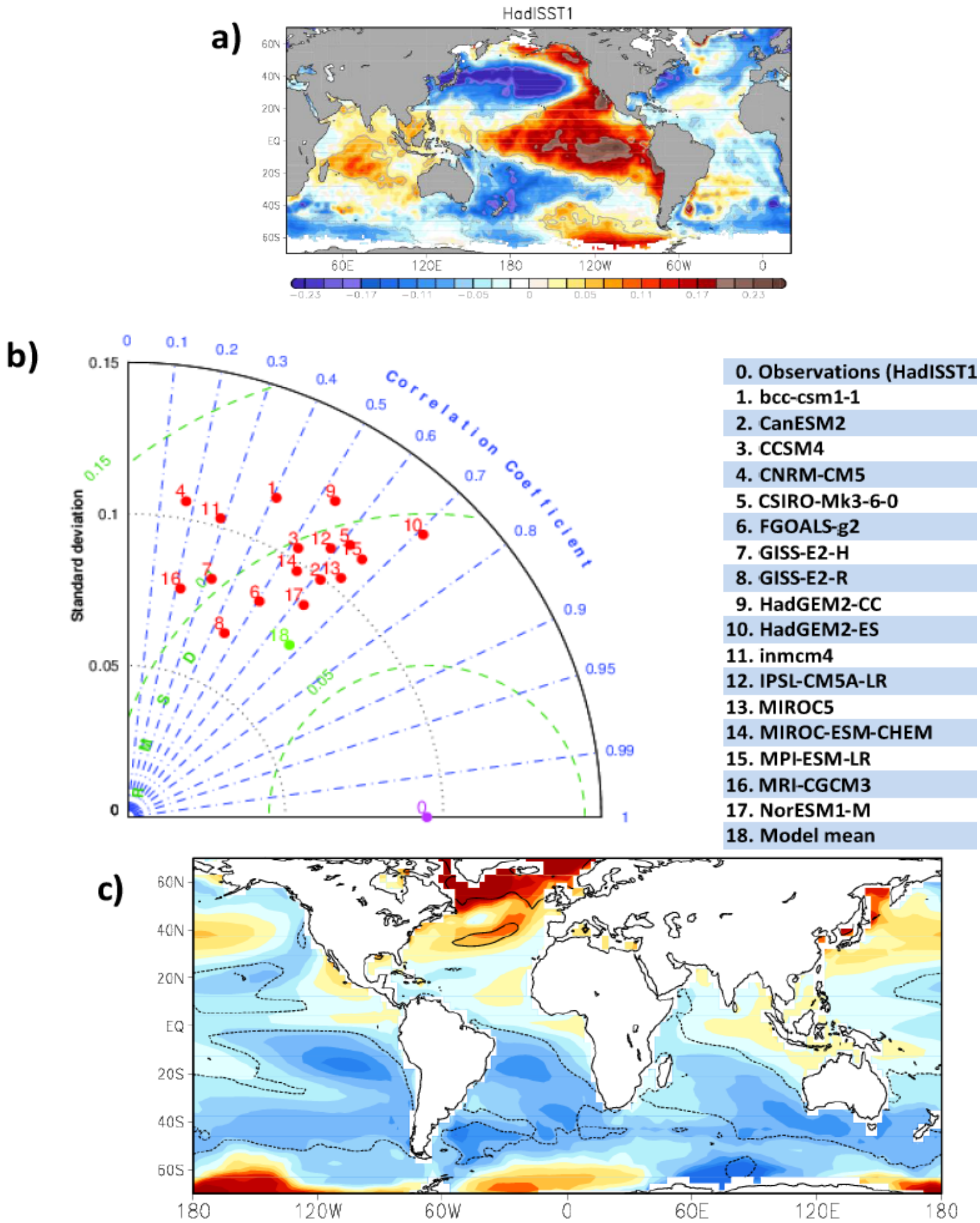


Figure 1.a.7:**(a)** Regression pattern of SSTA onto the observed IPO index (K/std. dev.) defined in VM15, using HadISST1data.**(b)** Taylor diagram comparing the IPO pattern of SSTA from observed HadISST1 data (purple dot) against the reproduced by CMIP5 models (red dots from 1 to 17 in the table at right) and the model-mean pattern (green dot) from piControl simulations. Correlation coefficients greater than r=0.48 are statistically significat at 95% according to a Student t-test. **(c)** Biases of the annual-mean SSTA of the climatology of the 17 CMIP5 models, with respect to the observed (avegraged from year 1910 to 2004), regressed onto the index of correlation coefficients between the observed and the simulated IPO patterns represented in the Taylor diagram above. Black contous indicates where the correlation is significant at a 90%.

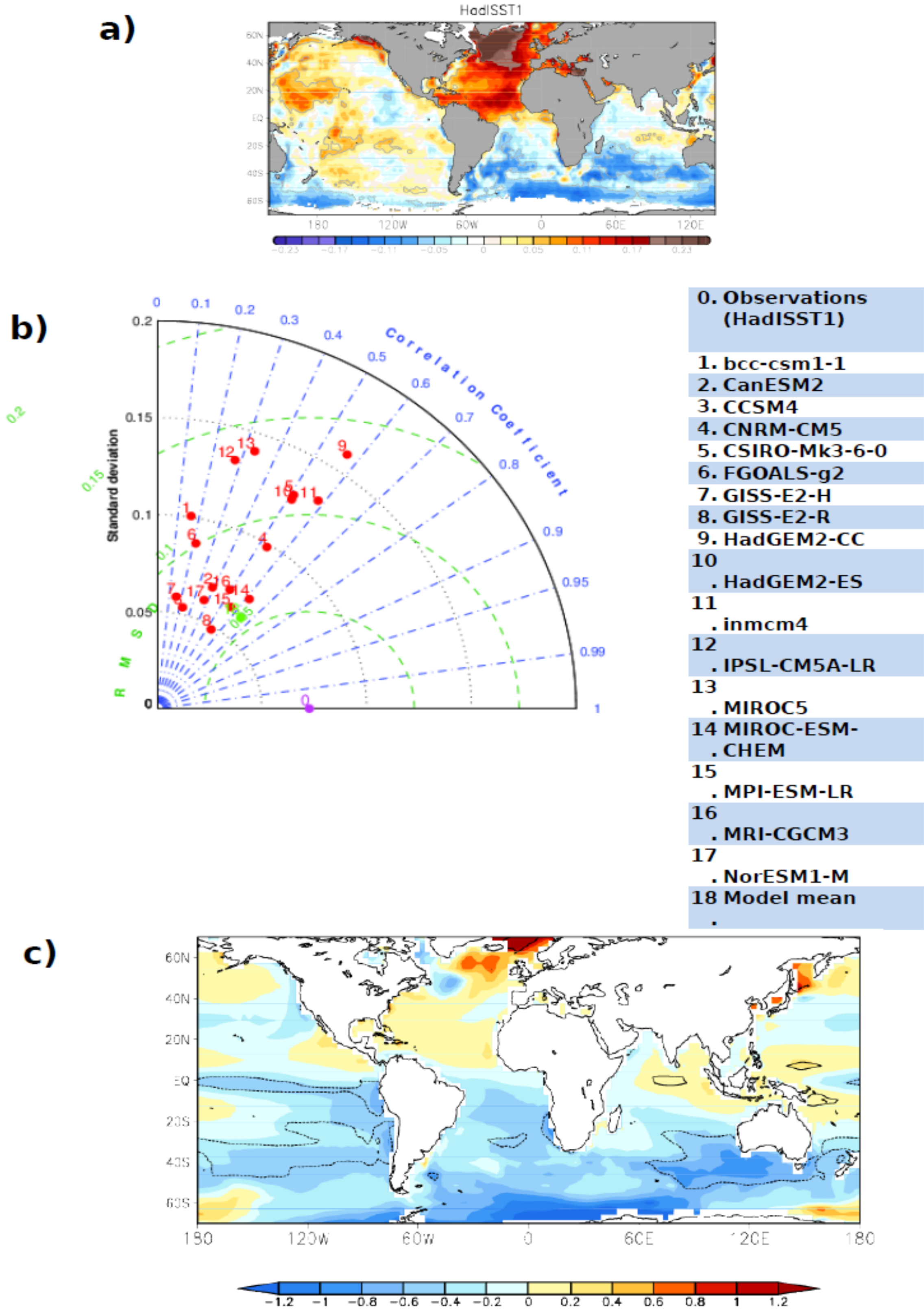


Figure 1.a.8: Same as Figure 1.a.7 but for the AMO patterns for SSTA

On the other hand, the simulated Atlantic Multidecadal Oscillation (AMO) patterns, calculated with the same models and methods as in VM15 applied to the North Atlantic SSTA, are less correlated to the observed one than the IPO (Figure 1.b.9). Moreover, the skill in simulating the AMO patterns is not as strongly linked to the bias as in the IPO case, since the regression map is similar but not statistically significant (Figure 1.b.9.c).

The arisen ideas of these preliminary results are currently being addressed in a deeper analysis which is expected to be published in the near future.

**Hypothesis posed:**

There are two main ways in which the mean state of SST is represented in CMIP5 models. One in which some models present a warmer southern hemisphere ocean in relation to less cloudiness in the extratropical southern hemisphere (and the opposite); and a second one in which the extratropical north Atlantic and the equatorial Pacific are colder (warmer) in relation with less cloudiness in the tropics.

Depending on this mean state the representation of the modes of variability changes among models, not only regarding its spatial configuration but also in the percentage of variability explained by each mode.

The idea is to perform sensitivity experiments in which the reduction of bias is achieved by enhancing the cloudiness in some regions of the SH extratropical areas.

In the next section, the results from a first set of sensitivity experiments done in coordination between the UCM , UCLA and UiB in relation to these hypothesis are presented.

### *1.2 To perform sensitivity studies*

**a) Influence of enhanced cloudiness in the extratropical Southern Hemisphere on the tropical bias (UCM in coordination with UiB) (Losada et al., 2015)**

**Participants:**

Teresa Losada Doval (UCM)
Roberto Mechoso (UCLA)
Antonio Castaño (UCM)
Shunya Koseki (UiB)
Elsa Mohino (UCM)
Belen Rodríguez-Fonseca (UCM)
Noel Keenlyside (UiB)

Based on the studies of Hwang and Friedson (2013) and Li and Xie (2014), and on the analysis of CMIP5 simulations performed in the previous section (Figure 1.b.2), sensitivity experiments with two different models have been made to test the influence of enhanced cloudiness in the extratropical Southern Hemisphere on the tropical biases.

**1. Introduction**

The eastern tropical and subtropical oceans are regions characterized by intense coastal upwelling that cools the ocean surface, and large-scale atmospheric subsidence of warm and dry air. Such conditions prevent deep convection to occur and favour the development of shallow stratocumulus clouds. The southeastern oceans show, thus, large and persistent stratocumulus cloud deck, extending from the Angolan-Namibian coast of Africa to the equator and from the coast of South America to almost 2000 km to the west in the Pacific (Klein and Hartmann, 1993). The stratocumulus deck, in turn, reduces the amount of incoming shortwave radiation, enhancing the initial cooling of the ocean. The upwelling drives ocean biological productivity, which is of great economic importance to the countries in the region.

Almost all CGCMs fail to reproduce the eastern boundary conditions, showing a warm bias in the eastern SSTs in both the tropical Atlantic and Pacific oceans that exceeds 2ºC in some regions (Richter, 2015). Also, most of the models show a reversal of the SST gradient in the equatorial Atlantic (Richter et al., 2014).

The SST bias is tightly related to the stratocumulus bias of CGCMs. Lin et al., (2014) shows that CMIP-5 models still have significant difficulty in simulating stratocumulus clouds and the associated cloud feedback in the Pacific; the models tend to simulate significantly less cloud cover, higher cloud top, and unrealistic cloud albedo. Such errors lead to excessive shortwave radiation at the ocean surface and to the increase of the underlying SST. Regarding the Atlantic, CMIP5 models also fail to fairly simulate the stratocumulus deck off the African coast. This failure leads to a misrepresentation of the radiative fluxes, as found for NCEP in Hu et al. (2008).

The second tropical bias present in every CMIP5 CGCM (Oueslati and Bellon, 2015) is the well-known double Inter-Tropical Convergence Zone (ITCZ) problem (Mechoso et al. 1995). The ITCZ can be identified as the tropical belt of deep convective clouds that is located on average around 6ºN latitude (Schneider et al., 2014). It is also identified as the region of maximum annual mean of precipitation (Philander et al., 1996). During boreal spring, the ITCZ shows a second maximum of rainfall in the southern Pacific. This second maximum is overestimated by CGCMs, which simulate a maximum in the southern Pacific during at least half of the year (Zhang 2001). A similar overestimation of precipitation appears in the Atlantic ocean. Because of this, the annual mean precipitation of CGCMs show a second maximum south of the equator in the Pacific and Atlantic oceans known as the double-ITCZ.

Despite the importance of the local processes, recent work has suggested that improving the simulation of regional processes may not suffice for an overall better CGCM performance, and that the effects of remote biases may override them. Remote biases with possible impact on the tropics are the deficient representation of clouds in the Southern Ocean (Hwang and Frierson, 2013; Li and Xie, 2014) and of the Atlantic Meridional Overturning Circulation (AMOC, Wang et al., 2014)

Regarding the former, Hwang and Frierson (2013) show that model biases even far away from the tropics can be linked to those in the tropics through changes in the Hadley circulation as result of the errors in atmospheric heating. On its part, Li and Xie (2014) reported that the link between the double-ITCZ problem and the bad representation of clouds in the Southern Hemisphere in CMIP-5 models could be established through the wind-evaporation-SST feedback (Xie and Philander, 1994). These arguments have been used to attribute the double ITCZ problem of CGCMs to cloud biases over the Southern Ocean.

In this work, we propose to improve the current knowledge of the impact of the extratropical bias of clouds in the Southern Hemisphere in the simulation of the main characteristics of tropical climate and its variability. The main hypothesis is that the improvement in the representation of the Southern Hemisphere (SH) cloudiness will improve the tropical biases of the CGCMs.

To this aim, we analyze idealized model experiments with two CGCMs, in which the shortwave radiation reflected by the clouds in the extratropical SH will be artificially increased, and we compare them with a control simulation.

## 2. Models and Experiment

### UCLA-MIT CGCM

UCLA-MIT CGCM is an ocean-atmosphere coupled global circulation model comprised by the UCLA-AGCM v7.1+SsIB (Mechoso et al., 2000; Ma et al., 2013) coupled to the MIT-OGCM (Marshall et al., 1997).

The atmospheric global circulation model **UCLA-AGCM** is a state of the art atmospheric model that covers the atmosphere from surface up to 50km high. The differentiation of the primitive equations is performed in an Arakawa-C grid. It uses a sigma vertical coordinate up to 1 mb, with 29 levels (14 in the stratosphere). The horizontal resolution of the model is 2º latitude by 2.5º longitude. The version of the model that will be used in this project has the **Simplified Simple Biosphere Model** (SSIB; Xue et al., 1991) incorporated. It is a surface model with three soil layers and one vegetation layer that gives the AGCM fluxes of momentum, sensible and latent heat, temperature and albedo. The scheme is integrated in the model as a component of the AGCM.

The ocean global circulation model **MIT-OGCM** covers a latitudinal domain form 80ºS to 79ºN. It has a horizontal resolution of 1º longitude. The meridional resolution is 0.3º between 10ºS-10ºN, increasing up to 1º out of the tropics. It has 46 vertical levels to a maximum depth of 5815 m. The model grid is 360x224x46. The integration time-step is also 1 hour. More details on the model can be found in Marshall et al. (1997).

### NorESM

Atmospheric component: Version 4.0 of Community Atmospheric Model (CAM4). 2.5deg by 1.9deg, and 23 vertical layers (pressure-coordinate).

Ocean component: Miami Isopycnal Coordinate Model (MICOM). 2Deg by 1deg with 53 vertical layers (isopycnal-coordinate)

Land component: Community Land Model (CLM4)

Sea Ice component: Los Alamos Sea Ice Model (CICE4)

Both experiments are initialised by historical run of NorESM (from 1850) and integrations for experiments start from 1980-01-01 and continue until 2004-12-31. All of results are 25-year climatology.

**Experimental set-up:**

COSZ is an idealized experiment that tries to simulate the effect that an improvement of the albedo of the clouds would have in the SW radiation and, thus, in the net radiation flux at the top of the atmosphere.

A modification in the incoming SW radiation is applied in the band between 30S-60S that reduces the incoming SW radiation there, with the maximum reduction at 45S (Figure 1).

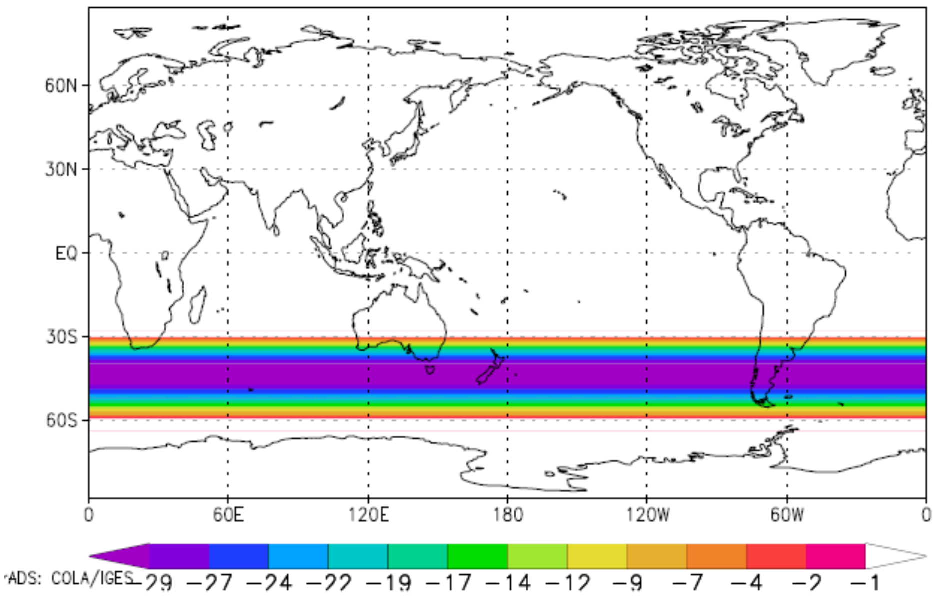


**Figure 1.c.1:** Reduction of SWD at TOA in COSZ.

The reduction of the incoming solar radiation has been applied by artificially modifying the cosine of the zenith angle at those latitudes (equation 1)

$$\text{Coszenth}=\text{coszenth}[1+ \alpha\sin(\text{lat}+30)\sin(\text{lat}+60)] \qquad \text{(equation 1)}$$

with $\alpha=1.5$.

The results of COSZ are compared with a control simulation (CTL). This modification can be interpreted as an increase of the albedo of the southern hemisphere clouds. That is, the SW incoming radiation is the same in COSZ than in CTL, and the SW outgoing radiation at the top of the atmosphere in COSZ is artificially increased by an amount equal to the one in Figure 1.c.1.

**UCLA-MIT CGCM Results**

Figure 1.c.1 shows the annual mean for the net radiation at the top of the atmosphere (TOA) for NCEP reanalysis (top) and control (CTL) simulation (center), along with the difference between the sensitivity experiment (COSZ) and CTL (bottom). The model has a clear overestimation of the net

radiation at TOA in almost the whole globe. This is more clearly shown in Figure 1.c.2, which depicts the annual mean of the zonal averaged net radiation at TOA for NCEP and simulations, together with the differences between simulations. Figure 1.c.2 shows that the two simulations overestimate the net radiation at TOA everywhere south of 60ºN.

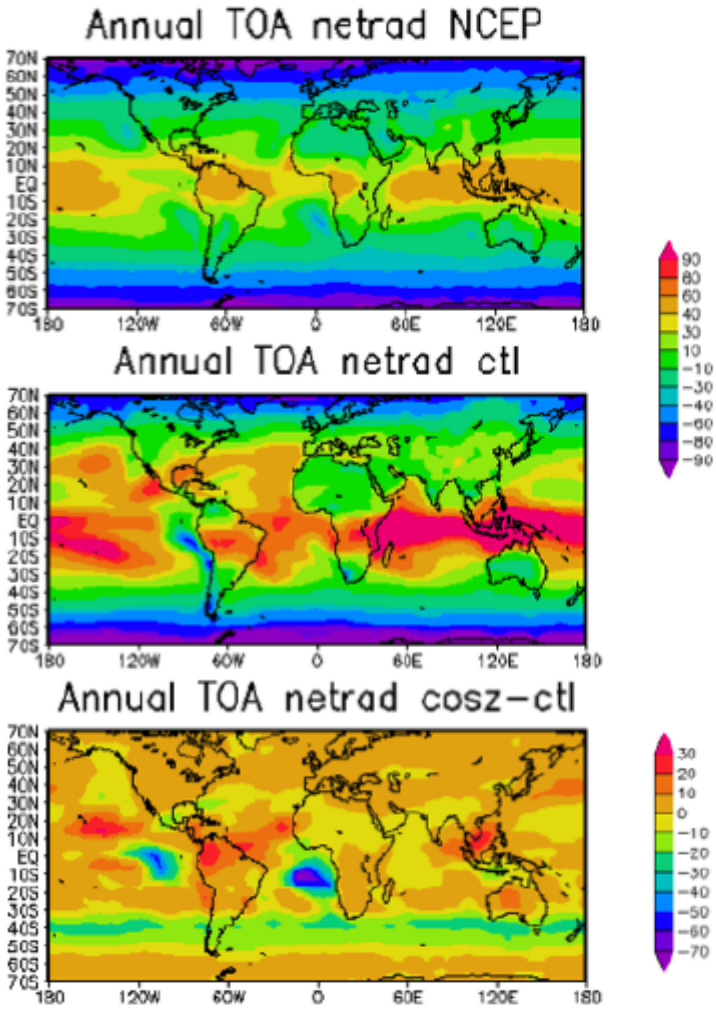


**Figure 1.c.2:** Annual net radiation at TOA for NCEP (top) and CTL (middle). Difference between net radiation at TOA in COSZ and CTL (bottom).

Looking at Figures 1.c.1 and 1.c.2, we can see that the overestimation of the net radiation at TOA in CTL is not symmetrical with respect to the Equator. The overestimation of the net radiation at TOA is stronger in the southern hemisphere (SH) than in the northern hemisphere (NH).

There is a clear reduction of the southern hemisphere (SH) overestimation in COSZ simulation, due to the reduction of outgoing SW radiation artificially applied between 30ºS-60ºS (Figure 1.c.1, bottom; Figure 1.c.2, right); but also due to a strong reduction of the net radiation at TOA in the subtropical southeastern Pacific and Atlantic Oceans, together with a slight increase of the incoming net radiation in the northern subtropics (Table 1.c.1).

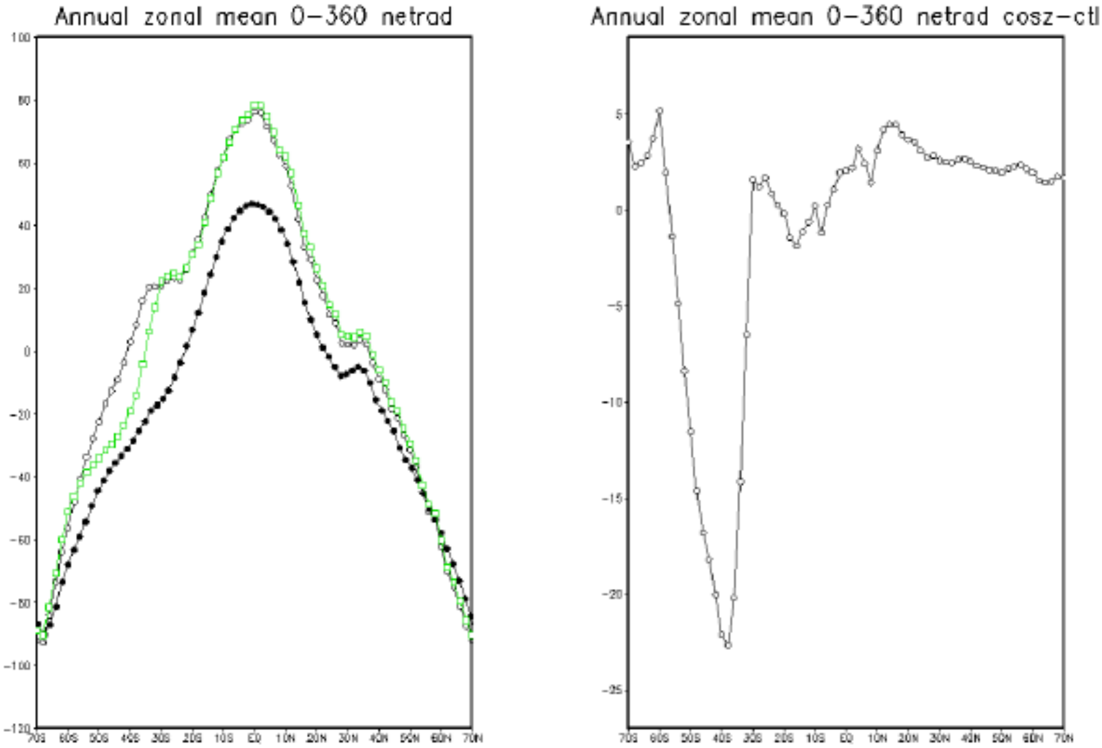


**Figure 1.c.3:** left) Annual mean of the zonally averaged net radiation at TOA for NCEP (black circles), CTL (black open circles) and COSZ (green cicles). Right) Differences of annual mean zonally averaged net radiation at TOA between COSZ and CTL.

| MEAN NET RADIATION AT TOA | NH | SH |
|---|---|---|
| CTL | 11,19 | 15,92 |
| COSZ | 13,20 | 5,15 |
| COSZ-CTL | -1,1 | -2,26 |

**Table 1.c.1:** Mean annual net surface radiation at TOA for NH (0-70N) and SH (0-70S) in CTL and COSZ; and difference between COSZ and CTL.

Table 1.c.2 shows the mean annual surface temperature for the NH and SH in observations, CTL and COSZ. The mean surface temperature is higher in the simulations than in the observations. The surface temperature is reduced in COSZ for both hemispheres, consistent with a reduction of the energy entering the system in COSZ. The reduction is stronger in the Southern hemisphere, as expected.

| MEAN AIR SURFACE TEMPERATURE | NH | SH |
|---|---|---|
| Observations | 14,78 | 13,59 |
| CTL | 17,64 | 16,55 |
| COSZ | 16,54 | 14,28 |
| COSZ-CTL | -1,1 | -2,26 |

**Table 1.c.2:** Mean annual surface temperature for NH (0-70N) and SH (0-70S) in observations, CTL and COSZ; and difference between COSZ and CTL.

We have shown in Figure 1.c.1 that the strongest reduction in the net radiation at TOA in COSZ is located in the southeastern Atlantic and Pacific, away from the region that receives less energy (30ºS-60ºS). It is well known that those are regions in which stratocumulus clouds form due to the presence of cold SST and subsiding warm air that prevents convection to occur. Figure 1.c.4 show the coverage of stratus clouds in the observations, CTL and the difference between COSZ and CTL. The model shows a deficiency in the simulation of the stratocumulus decks in the upwelling regions (California, Canarias, Angola, Perú) that is common for all the current CGCMs. The only region in which the stratus are well represented to some extent is the southeastern Pacific region.

COSZ simulation improves the representation of the stratus clouds in the Atlantic sector of the SH. However, it overestimate them in the southeastern Pacific, where the CTL simulation already have a fairly good representation of the stratrocumulus deck.

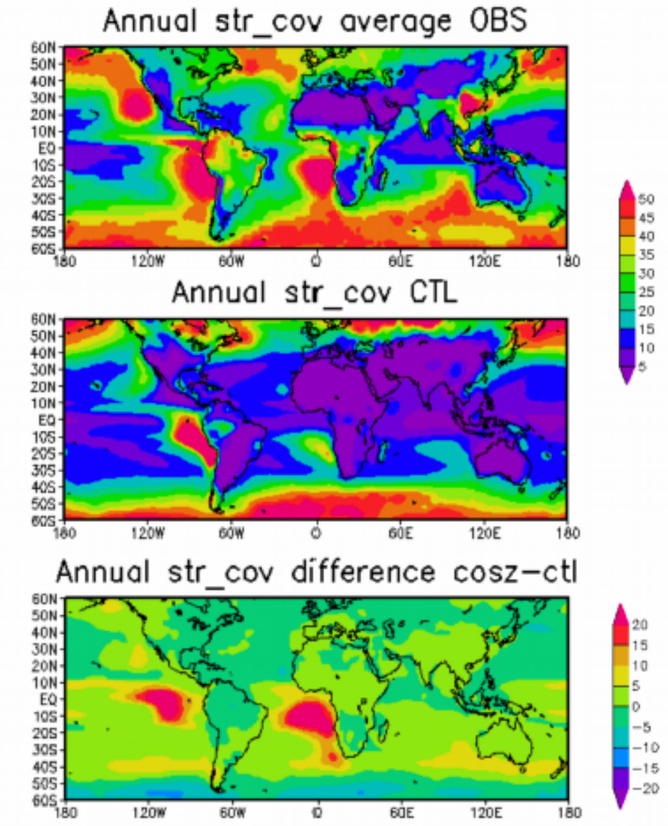


**Figure 1.c.4:** Annual stratus coverage for obs (top) and CTL (middle). Difference between stratus coverage in COSZ and CTL (bottom).

The impact of the reduction in the SH shortwave radiation on global SST can be seen in Figure 1.c.4. The model shows a clear overestimation of the SST in the tropical oceans in CTL (Figure 1.c.5, middle). In particular, CTL simulation shows a reversal of the zonal SST gradient in the equatorial Atlantic, a feature that is present in many of the current CGCMs (Richter et al., 2015). Once the modification of the shortwave radiation is applied, the SST is reduced everywhere in the globe except in the northwestern Pacific (Figure 1.c.5, bottom). This general cooling is consistent with the reduction in the total energy entering the system. What is more important is the pattern of the SST anomalies (COSZ-CTL difference).

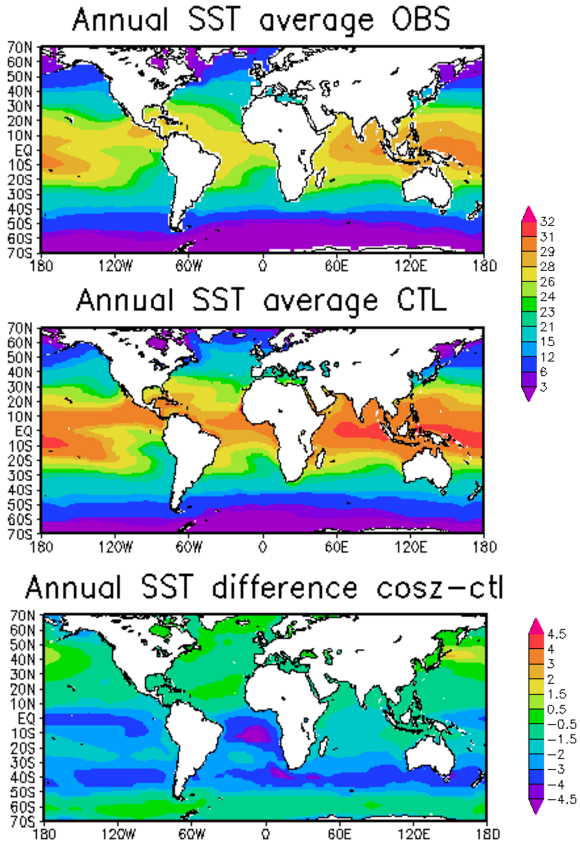


**Figure 1.c.5:** Annual SST for obs (top) and CTL (middle). Difference between SST in COSZ and CTL (bottom).

As one would have expected, the reduction is strongest in the southern hemisphere, where in fact the reduction is too strong (up to -4.5 degrees in some regions, where the maximum bias only reaches around 3 degrees). It is worth noting that the reduction of the SST in the subtropical southern Atlantic and Pacific is of the same order of magnitude than the one in the extratropics. This point to an important feedback between the subtropical SST and the stratocumulus clouds: The reduction in the SW radiation in the extratropical SH produces a decrease of the SST there. The cooler SST are then advected to the subtropics by the ocean gyres. The cooling of the subtropical SST produces an increase in the stratocumulus deck that, in turn, cools further the subtropical southern oceans.

The overestimation in the reduction of SST may be due to the decrease in the global amount of energy entering the system. To do a first order quantification of how much of the SST reduction is produced by the decrease in the SW radiation, we can subtract to the anomalies the global annual mean difference between CTL and COSZ, which is 1.68 degrees. Even doing so, the cooling in the SH would be still too intense over the south-tropical Atlantic.

Overall, the SST anomalies show an anomalous South-North gradient that would affect the position of the ITCZ. It is also striking that there response in the Indian Ocean is weak, where the stratus response is also very weak.

The impact of the SW reduction in precipitation is shown in Figure 1.c.6. COSZ experiment shows a clear reduction of the wet bias in the Pacific around 10S-30S, and also in the equatorial band of the Atlantic and eastern Pacific sectors. Nevertheless, the reduction of precipitation is too strong in the equatorial western Pacific and in the Maritime Continent sector.

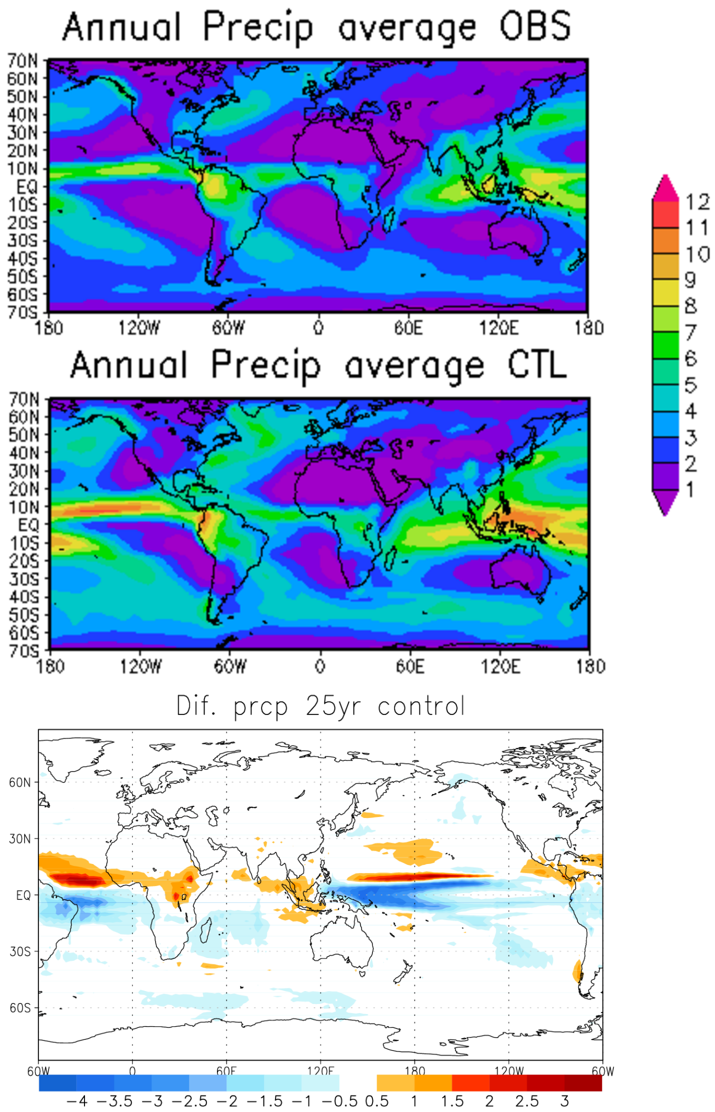


**Figure 1.c.6:** Annual precipitation for obs (top) and CTL (middle). Difference between precipitation in COSZ and CTL (bottom).

The results depicted so far point to a global influence of the reduction of the extratropical southern cloud bias. Such reduction would produce a decrease in the SST in the SH and a South-North gradient of temperature that would lead to the northward migration of the ITCZ.

**Nor-ESM Results**

The same simulations have been done with a second CGCM: the Norwegian Nor-ESM model.

The reduction in the incoming SW radiation produces a reduction of the mean annual SST in the whole globe except in the northwestern Pacific (Figure 1.c.7), with maximum reduction in the SH. But, unlike in UCLA-MIT, the reduction of the subtropical SST in NorESM is weaker than the extratropical one.

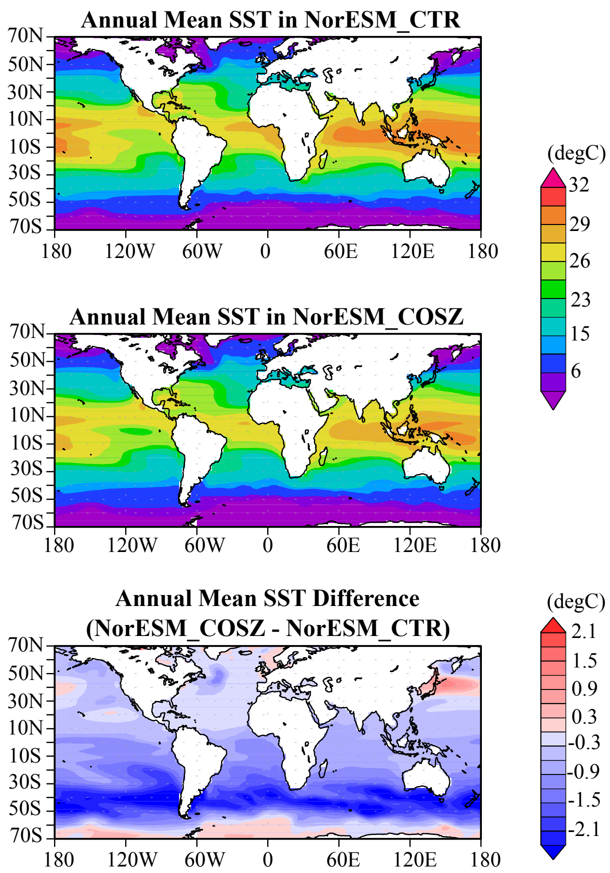


**Figure 1.c.7:** Annual SST for CTL (top) and COSZ (middle) in NorESM. Difference between SST in NorESM COSZ and CTL (bottom).

Accordingly with the meridional gradient of SST, the ITCZ moves to the north in COSZ experiment (Figure 1.c.8).

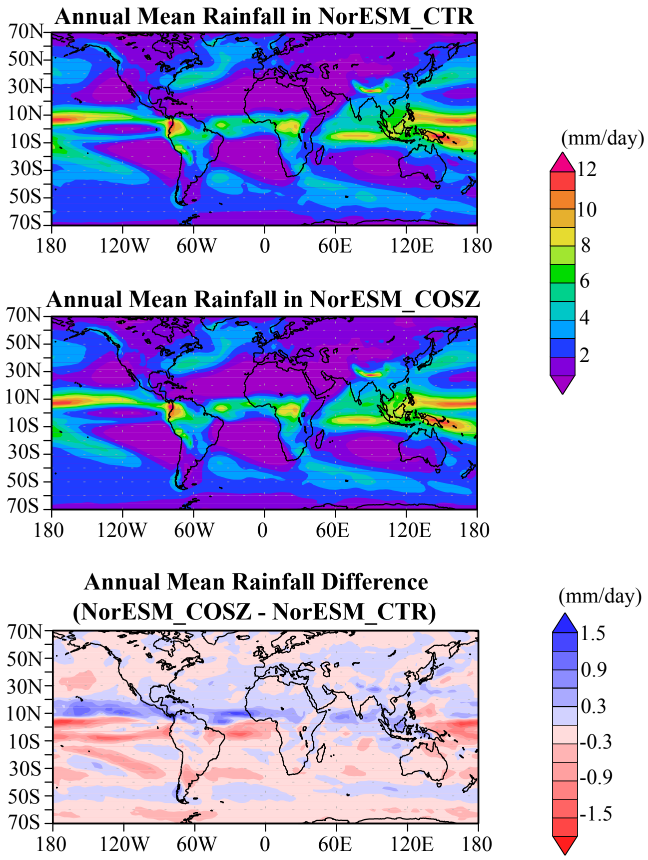


**Figure 1.c.8:** Annual precipitation for CTL (top) and COSZ (middle) in NorESM. Difference between precipitation in NorESM COSZ and CTL (bottom).

Figure 1.c.9 shows the response of the low level clouds in NorESM. It is necessary to take into account the fact that, on the contrary to UCLA-MIT model, NorESM doesn't have an output for the stratus clouds, and we are showing here the total low level cloudiness. It is clear that NorESM model doesn't reproduce the impact of the advection of cool SST to the subtropics into the low level clouds. As this model doesn't show the SST-stratus feedback, the cooling of the subtropical SST is less pronounced that in UCLA-MIT results.

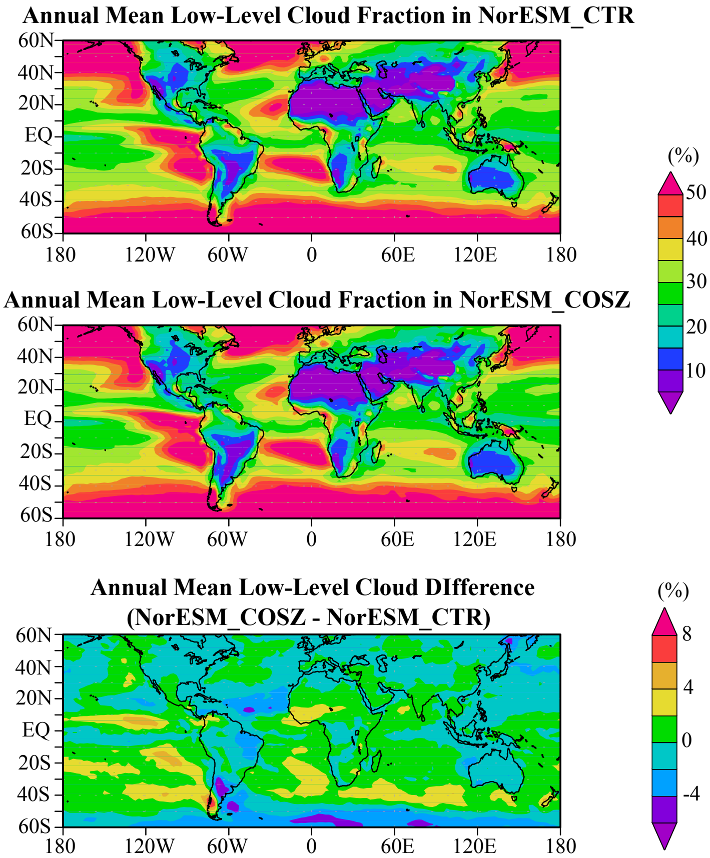


**Figure 1.c.9:** Annual low level clouds for CTL (top) and COSZ (middle) in NorESM. Difference between precipitation in NorESM COSZ and CTL (bottom).

**Conclusions**

Results shown here show that the artificial improvement of the southern ocean clouds have a strong impact in the tropical bias of SST and precipitation. The SST in the tropical and subtropical southern oceans is cooled by the advection of cool water from the southern extratropics and the interaction with the stratocumulus decks in the subtropical southeastern oceans seem to further enhance the cooling in the tropics and subtropics. The position of the ITCZ is better represented, with a northward displacement of the rainfall belt.

Based on the CMIP5 analysis done in Polo et al (2015, to be submitted), these simulations are going to be also used in the future to see if the improvement of bias enhance the representation of the interannual to decadal SST modes.

### 1.d) Influence of correcting north Atlantic sea surface salinity on tropical Atlantic bias (Park et al., 2015; Drews et al., 2015)

**Participants**

T Park (GEOMAR)
W Park (GEOMAR)
P. Greatbach (GEOMAR)
M. Latif (GEOMAR)

Different studies have been done to test the impact of remote bias on tropical Atlantic variability. GEOMAR has been working on this part performing different sensitivity experiments.

On the one hand, Park et al (2015) have study the influence of correcting the sea surface salinity (SSS) on the circulation of the North Atlantic as well as on the North Atlantic decadal to multidecadal variability (Figure 1.d.1). They have performed integrations of the Kiel Climate Model (KCM) with and without applying a freshwater flux correction over the North Atlantic. The quality of simulating the North Atlantic sector mean climate and decadal variability is greatly enhanced in the freshwater flux-corrected integration which, by definition, depicts relatively small North Atlantic SSS biases. In particular, a large reduction in the North Atlantic cold sea surface temperature (SST) bias is observed and a more realistic Atlantic Multidecadal Variability (AMV) simulated. Improvements relative to the non-flux corrected integration also comprise a more realistic representation of deep convection sites, sea ice, gyre circulation and Atlantic Meridional Overturning Circulation (AMOC). The results suggest that simulations of North Atlantic sector mean climate and decadal variability could strongly benefit from alleviating sea surface salinity biases in the North Atlantic, which may enhance the skill of decadal predictions in that region. However, the improvement in the representation of the AMOC does not enhance the simulation of the tropical Atlantic.

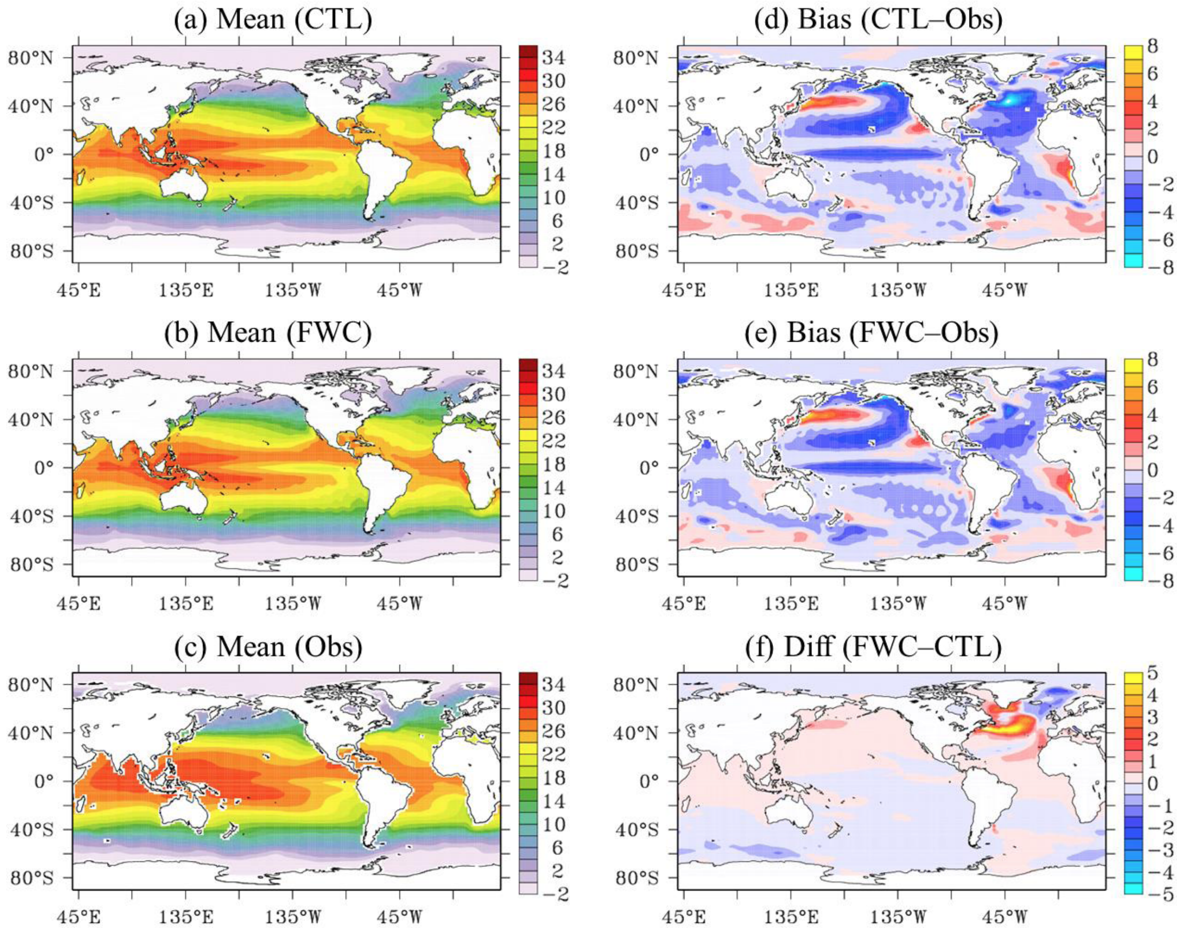


**Figure 1.d.1**: Long-term annual-mean SST (¡C) in (a) the control run, (b) the freshwater flux corrected integration, and (c) from Levitus climatology. SST biases (C) are depicted in (d) for the control run, (e) the freshwater flux-corrected integration, (f) depicts the difference in SST between the two integrations. (From Park et al., 2015).

Figure 1.d.1 also shows that the improvement in the North Atlantic does not improve the biases in the tropical Atlantic and Pacific oceans, indicating that a stronger AMOC does not reduce tropical Atlantic SST biases

GEOMAR has also studied the impact of the North Atlantic SST bias on the Tropical Atlantic bias (Drews et al., 2015), finding that the reduction of bias in this region does not affect the tropical bias.

## 2. To test the Influence of the TA bias on the representation of the mean state and variability outside of the Tropical Atlantic

In this section different simulations from Rodriguez-Fonseca et al (2009), Polo et al (2015) and Ding et al (2012) have been used to see the impact of the reduction of Atlantic bias on the Indo-Pacific bias and variability. The simulations differ in the flux correction applied and in the way the models have been set up. The different configurations of the simulations together with the different resolutions of the ocean and atmosphere from each of the models used can be used as an advantage to infer common results or differences that can help in the interpretation of the influence of bias on variability and viceversa.

The results have been divided based on the contribution done from UiB and GEOMAR (Ding et al. 2012 simulations) and that done from UCM (Rodriguez-Fonseca et al, 2009; Polo et al. 2015 simulations).

### 2.a Contribution from UiB and GEOMAR

N. Keenlyside (UiB)
H. Ding (GEOMAR)
M. Latif (GEOMAR)

Experiments with the ECHAM5/MPIOM coupled model show that mean errors in the tropical Atlantic are firstly associated with approximately 0.5°C warmer sea surface temperature (SST) over the entire tropics, as a result of the thermal warming of the entire troposphere. Secondly, the Atlantic SST errors strengthen the equatorial zonal SST gradient by approximately 1°C. These dynamically driven changes seem mediated by the SST errors in both the north and south tropical Atlantic.

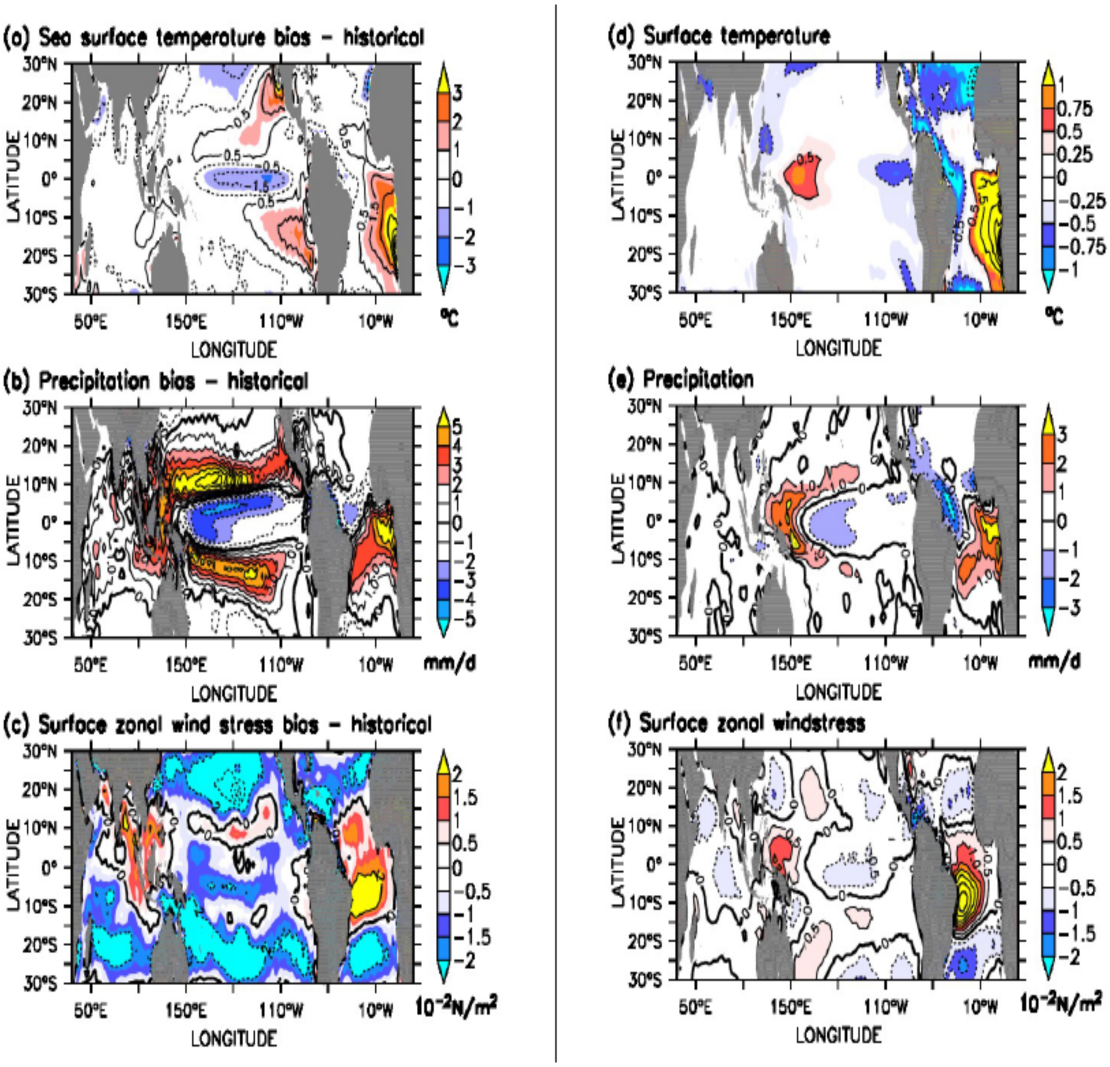


**Figure. 2.a.1:** Left panels show the mean error in (a) sea surface temperature, (b) precipitation, and (c) surface zonal wind stress in the Historical run, as compared to observations and considering the period 1980-2000. Right panels show the corresponding Historical minus Observed-Atlantic differences. For (d) the mean warming across tropics is removed to emphasis the dynamical driven changes.

The mean model errors are typical of most climate models (Fig. 2.a.1, a-c). In the Pacific, the equatorial cold tongue is approximately 2°C too cold, while there are warm SST biases at the coasts of North and South America. In the south Atlantic the SST error extend from the equator to the Angolan coast, where it exceeds 5°C. While SST in the north tropical Atlantic are approximately 0.5°C to cold. The SST errors are associated with excess precipitation in the South Atlantic and a strong double Intertropical Convergence Zone (ITCZ) error in the Pacific. The trade winds in the Atlantic appear to strong in the north and to weak in the south, consistent with the SST errors. In the Pacific the equatorial trade winds are biased easterly compared to the NCEP reanalysis.

The difference in the Historical minus Observed-Atlantic simulations provides an assessment of the impact of the tropical Atlantic SST biases on the simulation climate across the tropics. The Historical simulation is 0.46°C warmer than the Observed-Atlantic. This is because the warmer tropical Atlantic SST warms the tropical troposphere, and fast atmospheric wave adjustment transmits the signal across the tropics. This provides a thermal warming of ocean in regions remove from the Atlantic. Conversely, correcting the Atlantic SST errors would lead to a ~0.5°C cooler tropical SST.

The tropical Atlantic SST error also enhance the equatorial zonal SST gradient in the Pacific by around ~1°C (Fig. 1d). The equatorial zonal SST gradient between 165°E to 145°W and averaged over 5°S-5°N is 3.8°C in the observations, while in the Historical and Observed-Atlantic it is 4.4°C and 3.3°C, respectively. The changes in SST in the Pacific are associated with a westward displacement in precipitation over the western equatorial Pacific and a weak enhancement of the equatorial easterlies over the eastern Pacific by approximately 10% (Fig. 2.a.1, e-f).

Studies show that interannual variability of tropical Atlantic SST can drive a delayed response in the Indo-Pacific, with an equatorial Atlantic Niña in boreal summer associated with an El Niño like SST anomalies six months later (Rodriguez-Fonseca et al., 2009), and north tropical Atlantic cooling in boreal spring associated with a central Pacific Niño warming (Ham et al., 2013). Neither of these mechanisms seems to act in the evolution of seasonal errors. The equatorial Atlantic SST errors peak in July and August, while the largest differences between the Historical and Observed-Atlantic runs occurs in May and June (Fig. 2.a.2, a). The precipitation and zonal wind stress differences also tend to precede the peak in the equatorial Atlantic SST error (Fig. 2.a.2, b-c). Closer inspection of the Historical minus Observed Atlantic SST in boreal spring shows that the largest SST, precipitation, and zonal wind stress errors occur south of 5°S, but there are substantial errors in the north tropical Atlantic (Fig. 2.a.2, d-f). Furthermore, the errors in north tropical Atlantic appear linked to those in equatorial eastern Pacific.

Further work is underway to better diagnose the thermodynamic (e.g., wind-evaporative-SST feedback) versus dynamical driven changes in the Pacific response. Additional experiments to assess the relative contributions of the north versus south tropical Atlantic errors are being planned. The mean errors in the Atlantic also appear to impact the variability in the Pacific, and this will also be analysed further.

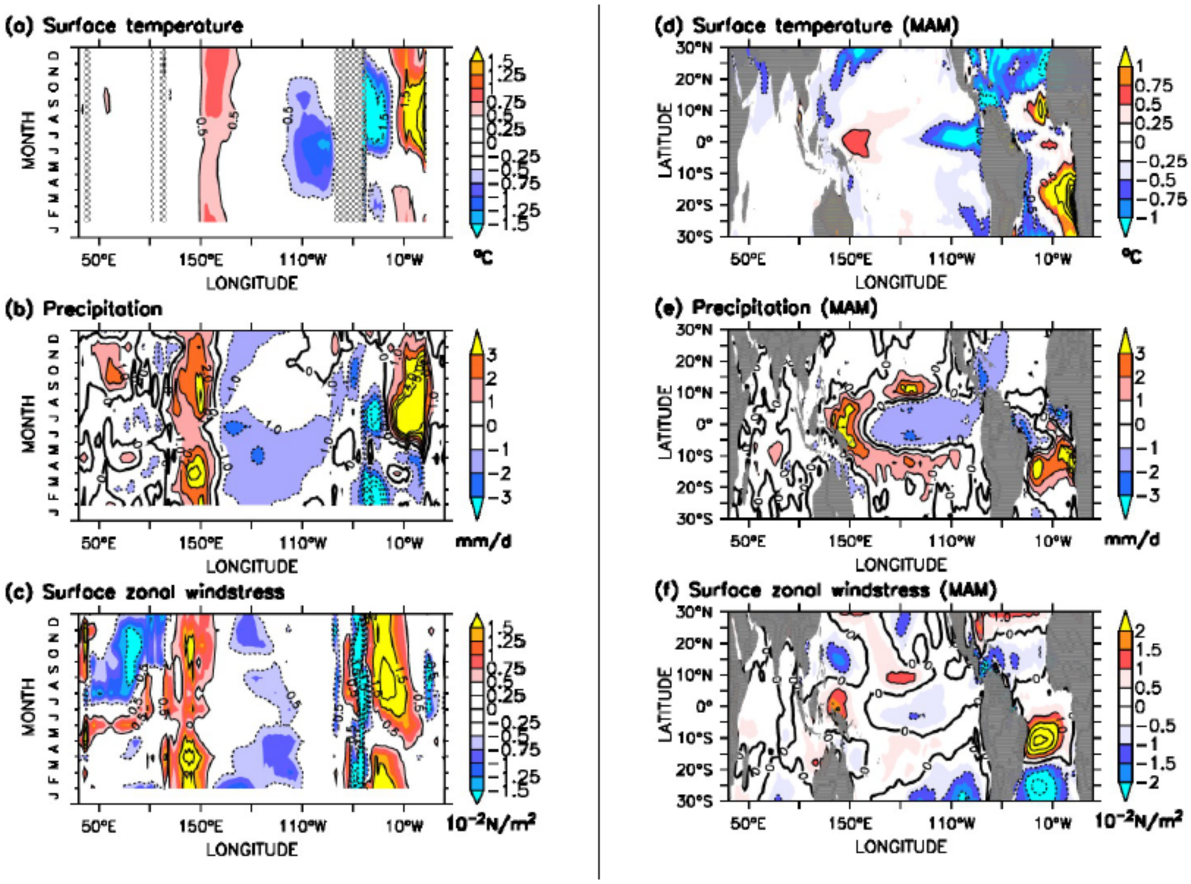


**Figure 2.a.2:** Left panels show the seasonal evolution of the Historical minus Observed-Atlantic differences in (a) sea surface temperature, (b) precipitation, and (c) surface zonal wind stress averaged between 5°S-5°N. Right panels show the corresponding spatial map averaged over March to May. For (a) and (d) the mean warming across tropics is removed to emphasis the dynamical driven changes.

## 2.b Contributions from UCM

Irene Polo (UCM)

Marta Martín Rey (UPMC)

Belén Rodríguez-Fonseca (UCM)

**Influence of Atlantic variability on Mean Bias and variability over Indo-Pacific**

Experiments with SPEEDY- coupled with RGO and NEMO models show that variability over the Atlantic basin is associated with an increase of variability over the whole equatorial band.

The variability over the Atlantic increases the cool mean bias over the Western Pacific and the Maritime continent by 0.16C for SPEEDY-NEMO, while for SPEEDY-RGO, theres is a reduction of the warm bias over the eastern Pacific. The differences in the region of impact could be due to the mean convection of the different models. In this context, more dynamical variables as wind stress and precipitation need to be analysed in a future work to understand this impact, taking into account that a flux correction is applied.

<u>Model experiments</u>

The CGCM used in this work is the AGCM SPEEDY model (version 41) coupled to two different ocean models. SPEEDY has 8 vertical levels, and the horizontal spectral truncation is T30. The model includes physically based parametrizations of large-scale condensation, shallow and deep convection, short-wave and long-wave radiation, surface fluxes of momentum, heat and moisture, and vertical diffusion (Kucharski et al., 2013).

We have two sets of simulations, SPEEDY model is coupled to i) NEMO V3.0 model (Madec 2008) which is a primitive equation z- level model making use of the hydrostatic and Boussinesq approximations. This version has a tripolar ORCA2 configuration with horizontal resolution of 2° and a tropical refinement to 1/2°. and 31 vertical levels. NEMO also includes a dynamic sea-ice model component (LIM; Fichefet et al. 1997). This simulations are described in Kucharski et al. (2015). ii) RGO (Chang 1994) 1.5 layers ocean model where only the first layer is dynamically active. The thermodynamic equation is also included in a fixed mixed layer to relate temperature variations with mixing, advection and surface heat fluxes (Chang 1994). This simulations are described in (Rodriguez-Fonseca et al., 2009).

A flux-correction is applied to climatological surface heat fluxes and wind stresses to reduce the model's drift. The flux correction approach employs a one-way anomaly coupling from the ocean to the atmosphere. The heat fluxes used by the ocean component are based on full SST, while heat fluxes that force the atmosphere are based on anomalies of SST (Kucharski et al., 2015)

A partial-coupled experiment with SST relaxed to observations (from HadiSST) in the Atlantic basin and extending over the period 1900-2009 for NEMO and 1949-2009 for RGO are performed (hereafter SimVarAtl). In these experiments the Indo-Pacific is coupled and there is climatological SST elsewhere.

The outputs from SimVarAtl are compared with a partial-coupled experiment with SST relaxed to climatology in the Atlantic basin (hereafter SimClimAtl). The climatology is 1970-2008 for NEMO and 1981-1990 for RGO.  We see difference for the period of the climatology.

Results

A set of simulations where the SST over the Atlantic basin varies (SimVarAtl) with the experiments with climatology over the Atlantic (SimClimAtl) are compared. For both, the RGO and NEMO ocean models, the inclusion of the variability over the Atlantic basins increases significantly the variability over the equatorial Indo-Pacific along the year. This increase is about 120% with respect to experiments with climatological SST over the Atlantic (figure 2.b.1, c-d). This increases goes up to 140% in boreal spring over the Eastern Pacific with NEMO (figure 2.b.1, d). The increase of variability over the equatorial pacific due to the variability over the Atlantic is in agreement with previous results from (Martin-Rey et al., 2012; Kucharski et al., 2015)

Also, the change in the mean SST bias over the equatorial band has been checked. For RGO experiments, the variability over the Atlantic seems to reduce the warm bias along the central-eastern equatorial Pacific along the year, with maximum reduction between June-August (figure 2.b.1, a). This time of the year coincides with the maximum variability over the equatorial Atlantic, which suggests connection between Niños (Rodriguez-Fonseca et al., 2009).

However, for SPEEDY-NEMO, the variability over the Atlantic produces a significant, although small, increase of the cold change  (-0.16C) over the west Pacific and Maritime continent (figure 2.b.1, b) when consider the variability over the Atlantic.

The change in the mean bias is therefore, model dependent, suggesting that the mean state has to be important in setting up the mean bias through local variability (i.e. feedbacks over different regions over Indo-Pacific).  The fact that the variability over the Atlantic could affect remote mean bias over the Indo-Pacific highlights the importance of a proper Atlantic simulation for predicting ENSO. The effect of the inclusion of the mean bias over the Atlantic in these relationships needs to be explored with further control simulations.

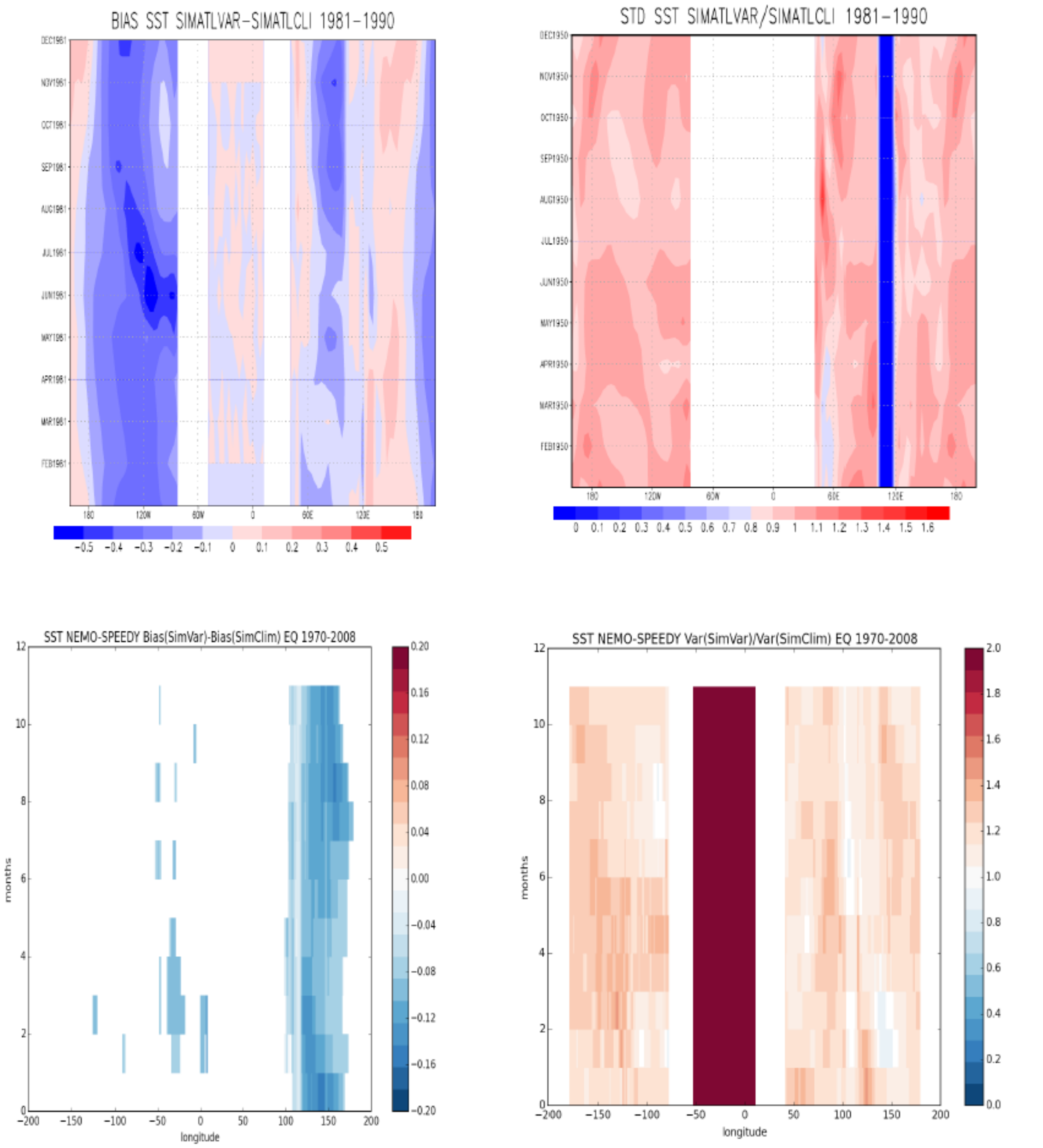


**Figure 2.b.1.** Left: Mean SST bias along the Eq. between SIMATLVAR and SIMATLCLI for SPEEDY-RGO (top,a) and SPEEDY-NEMO (bottom,b). Right: Ratio between the std of the SST between SIMATLVAR and SIMATLCLI from SPEEDY-RGO(top,c) and SPEEDY-NEMO (bottom,d). Significant for SPEEDY-NEMO with ttest and F-test with alpha=0.1

**References** (Blue references are papers within the PREFACE project)

Ding, H., N. Keenlyside, and M. Latif, 2012: Impact of the Equatorial Atlantic on the El Niño Southern Oscillation. *Climate Dynamics*, **38,** 1965-1972.

Hu ZZ, Huang B, Pegion K (2008) Low cloud errors over the southeastern Atlantic in the NCEP CFS and their association with lower-tropospheric stability and air-sea interaction. *J. Geophys. Res.*, **113**, D12114.

Hwang, Y.-T. and D. M. W. Frierson, 2013: Link between the double-Intertropical Convergence Zone problem and cloud biases over the Southern Ocean. *Proceedings of the National Academy of Sciences*, **110,** 4935-4940.

Drews A, Greatbatch RJ, Ding H, et al. (2015) The use of a flow field correction technique for alleviating the North Atlantic cold bias with application to the Kiel Climate Model. *Ocean Dynamics,* **65**, 1079–1093. doi: 10.1007/s10236-015-0853-7

Klein SA, Hartman DL (1993) The seasonal cycle of low stratiform clouds. *J. Clim.*, **6**, 1587-1606.

Li, G. and S.-P. Xie, 2012: Origins of tropical-wide SST biases in CMIP multi-model ensembles. *Geophysical Research Letters*, **39,** L22703.

Lin JL, Qian T, Shinoda T (2014) Stratocumulus Clouds in Southeastern Pacific Simulated by Eight CMIP5–CFMIP Global Climate Models. *J. Clim.*, **27**, 3000-3022.

——, 2014: Tropical Biases in CMIP5 Multimodel Ensemble: The Excessive Equatorial Pacific Cold Tongue and Double ITCZ Problems. *Journal of Climate*, **27,** 1765-1780.

Losada T, Mechoso CR, Castaño A, Rodríguez-Fonseca B, Koseki S, Mohino E, Keenlyside N (2015) Impact of the bias in the extratropical southern ocean clouds in tropical biases in CMIP5 models. (In preparation).

Ma HY, Xiao H, Mechoso CR, Xue YK (2013) Sensitivity of Global Tropical Climate to Land Surface Processes: Mean State and Interannual Variability. *J. Clim.*, **26**, 1818-1837.

Marshall J, Adcroft A, Hill C, Perelman L, Heisey C (1997) A finite-volume, incompressible Navier Stokes model for studies of the ocean on parallel computers. *J. Geograph. Res., **102**, 5753–5766.*

Martin-Rey M, I. Polo. B. Rodriguez-Fonseca, T. Losada and A. Lazar (2015), On the different configurations of the Atlantic Nino phenomenon under negative AMO phases. - to be submitted

Mechoso CR, Robertson AW, Barth N, Davey MK, Delecluse P, Gent PR, Ineson S, Kirtman B, Latif M, Le Treut H, Nagai T, Neelin JD, Philander SGH, Polcher J, Schopf PS, Stockdale T, Suarez MJ, Terray L, Thual O, Tribbia JJ (1995) The seasonal cycle over the tropical pacific in coupled ocean–atmosphere general circulation models. *Mon. Weather Rev.*, **123**, 2825–2838.

Mechoso CR, Yu JY, Arakawa A (2000) A coupled GCM pilgrimage: from climate catastrophe to ENSO simulations. In: Randall DA (ed) General Circulation Model Development: past, present and future. Proceedings of a symposium in honor of Professor Akio Arakawa. Academic, New York, pp 539–575.

Nnamchi, H. C., J. Li, and R. N. C. Anyadike (2011), Does a dipole mode really exist in the South Atlantic Ocean? J. Geophys. Res., 116, D15104, doi:10.1029/2010JD015579.

Park T., W. Park, and M. Latif  Correcting North Atlantic Sea Surface Salinity Biases in the Kiel Climate Model: Influences on Ocean Circulation and Atlantic Multidecadal Variability , 2015 (submitted to Climate Dynamics)

Philander SGH, Gu D, Halpern D, Lambert G, Lau NC, Li T, Pacanowski RC (1996) Why the ITCZ is mostly north of the equator. *J. Clim.*, 9, 2958-2972.

Polo I., B. Dong and R. Sutton (2013) Changes in tropical Atlantic interannual variability from a substantial weakening of the meridional overturning circulation. Clim. Dyn., DOI 10.1007/s00382-013-1716-x

Polo, I., M. Martin-Rey, B. Rodriguez-Fonseca, F. Kucharski, and C.R. Mechoso, 2015: Processes in the Pacific La Niña onset triggered by the Atlantic Niño. *Climate Dynamics*, **44**, 115-131

Polo I, Julian Villamayor, Belen Rodriguez-Fonseca, Elsa Mohino Harris , Teresa Losada Doval, 2015. Bias and Variability at Interanual to Decadal Timescales in  CMIP5  models (to be submitted)

Polo an co-authors (in preparation) Understanding the growth of the errors in seasonal hindcast and the dependency of the ENSO phases

Oueslati B, Bellon G (2015): The double ITCZ bias in CMIP5 models: interaction between SST, large-scale circulation and precipitation. *Clim. Dyn*., **44**, 585-607.

Rayner, N. A., D. E. Parker, E. B. Horton, C. K. Folland, L. V. Alexander, and D. P. Rowell (2003), Global analyses of sea surface temperature, sea ice, and night marine air temperature since the late nineteenth century, J. Geophys. Res., 108(D14), 4407, doi:10.1029/2002JD002670.

Richter I, Xie S-P, Behera SK, Doi T, Mausmoto Y (2014) Equatorial Atlantic variability and its relation to mean state biases in CMIP5. *Clim. Dyn.*, **42**, 171-188.

Richter I (2015) Climate model biases in the eastern tropical oceans: causes, impacts and ways forward. *WIREs Clim. Change*, **6**, 345–358.

Rodriguez-Fonseca, B., I. Polo, J. Garcia-Serrano, T. Losada, E. Mohino, C. R. Mechoso, and F. Kucharski, 2009: Are Atlantic Niños enhancing Pacific ENSO events in recent decades? *Geophysical Research Letters*, **36,** L20705.

Schneider T, Bischoff T, Haug GH (2014) Migrations and dynamics of the intertropical convergence zone. *Nature*, **513**, 45-53.

Taylor, K. E., R. J. Stouffer, and G. A. Meehl (2012), An overview of CMIP5 and the experiment design, Bull. Am. Meteorol. Soc., 93, 485–498.

Tozuka, T., T. Doi, T. Miyasaka, N. Keenlyside, and T. Yamagata, 2011: Key factors in simulating the equatorial Atlantic zonal sea surface temperature gradient in a coupled general circulation model. *Journal of Geophysical Research-Oceans*, **116**.

Villamayor, J., and E. Mohino (2015), Robust Sahel drought due to the Interdecadal Pacific Oscillation in CMIP5 simulations, Geophys. Res. Lett., 42, doi:10.1002/2014GL062473.

Wang, C., L. Zhang, S.-K. Lee, L. Wu, and C. R. Mechoso, 2014: A global perspective on CMIP5 climate model biases. *Nature Clim. Change*, **4,** 201-205.

Xie S-P, Philander SGH (1994) A coupled ocean-atmosphere model of relevance to the ITCZ in the eastern Pacifc. *Tellus A*, **46**, 340-350.

Xue Y, Sellers PJ, Kinter JL III, Shukla J (1991) A simplified biosphere model for global climate studies. *J, Clim.*, **4**, 345–364.

Zhang C (2001) Double ITCZs. *J. Geophys. Res. Atmos.*, **106**, 11785–11792.

Zhang, L., and C. Wang (2013), Multidecadal North Atlantic sea surface temperature and Atlantic meridional overturning circulation variability in CMIP5 historical simulations, Journal of Geophysical Research: Oceans, 118(10), 5772-5791.

**Acknowledgements:**

The contributors of this deliverable would like to acknowledge the collaboration and advice of Professor Carlos Roberto Mechoso from UCLA.

Also, we acknowledge the help of E. Exarchou and C. Prodhomme, from IC3 and S. Bush from UREAD for providing the hindcast data used in section 1a (table 1a).